JOURNAL OF GEOPHYSICAL RESEARCH, VOL. 92, NO. C4, PAGES 3691–3708, APRIL 15, 1987

Seasonal Cycle of Velocity in the Atlantic North Equatorial Countercurrent as Measured by Surface Drifters, Current Meters, and Ship Drifts

P. L. RICHARDSON

Woods Hole Oceanographic Institution, Woods Hole, Massachusetts

G. REVERDIN

Laboratoire d'Océanographie Dynamique et de Climatologie, Paris

This report describes the general circulation and seasonal variation of currents in the equatorial Atlantic, concentrating on the North Equatorial Countercurrent (NECC), using data collected as part of the Seasonal Response of the Equatorial Atlantic and Programme Français Océan et Climat dans l'Atlantique Equatorial experiments plus historical ship drifts. During 1983–1985 the Lagrangian circulation was studied by launching and tracking 30 freely drifting drogued buoys in the North Equatorial Countercurrent and 23 in the South Equatorial Current (SEC). In addition, continuously recording current meters were moored for 20 months at depths from 20 to 300 m near the center of the NECC, at 6°N, 28°W. These measurements are the longest series ever obtained in this current and provide information about its seasonal and interannual variations and zonal, meridional, and vertical structure. The seasonal cycle of the NECC is very regular from year to year. Each year the NECC starts up in May–June. It flows eastward across the Atlantic with surface speeds of up to 143 cm/s in the west, extending down to 350 m at 28°W, and flowing into both the Guinea Current and North Equatorial Current. It disappears or reverses from about January–June west of 18°W. Some near-surface water of the NECC is inferred to downwell and flow equatorward toward the Equatorial Undercurrent. The SEC flows into the North Brazil Current, which during spring continues up the coast into the Caribbean. During fall, however, the whole North Brazil Current retroflects, or turns back on itself, between 45° and 50°W, forming the western NECC. The retroflection establishes a meander pattern in the NECC that slowly propagates westward during fall at a speed of 4 cm/s. The meanders have a displacement of about 300 km in latitude, a wavelength of 900 km, and meridional velocity fluctuations of up to 100 cm/s. The swift currents and time-dependent meanders in the western NECC cause a high eddy kinetic energy, ~ 2400 cm^2/s^2, equivalent to that of the energetic part of the Gulf Stream.

1. INTRODUCTION

The Seasonal Response of the Equatorial Atlantic Experiment (SEQUAL) is an observational and theoretical study of the response of the upper layers of the equatorial Atlantic Ocean to the seasonally varying surface winds. This report describes results from the SEQUAL drifters program and a current meter mooring which measured surface and subsurface currents in the North Equatorial Countercurrent (NECC) during 1983–1984. Also included are some French buoys [*Reverdin and McPhaden*, 1986] and some historical ship drifts. The new data are the first direct velocity time series ever measured in the NECC over a complete seasonal cycle. The observations give information about the meridional, zonal, and vertical structure of the NECC; about sources and sinks of water flowing in the NECC; and about interannual, seasonal, and higher-frequency fluctuations.

Historical ship drifts show that the NECC is an intense eastward current which appears seasonally between 4°N and 10°N and is bounded by the North and South Equatorial currents (see Figure 1). The origin of the NECC is the North Brazil Current, part of which turns eastward during fall. In the east, the NECC flows into the Guinea Current.

Equatorial currents are very swift, transport large amounts of water, and have huge spatial and temporal variations. If one considers north-south sections through the Gulf Stream and through the equatorial currents, the mighty Gulf Stream appears quite frail compared with the swift South Equatorial Current (SEC) (Figure 2). In July the mean velocity of the near-surface NECC is almost identical to the mean Gulf Stream in amplitude and width. The NECC, however, disappears for half of the year.

Although the seasonal variability of the NECC was known qualitatively before SEQUAL from historical ship drifts [*Schumacher*, 1940, 1943; *Boisvert*, 1967], hydrography [*Cochrane et al.*, 1979], a few drifters [*Molinari*, 1983; J. D. Cochrane, personal communication, 1982], and brief current-meter moorings [*Bubnov et al.*, 1979; *Halpern*, 1980; *Perkins and Van Leer*, 1977], a quantitative picture was lacking owing to the sparseness of data and the lack of appropriate data over a complete yearly cycle. During SEQUAL, further analyses of historical data, including thermocline depth and wind stress [*Garzoli and Katz*, 1983] and ship drifts [*Richardson and McKee*, 1984; *Richardson and Walsh*, 1986], provided a better picture of climatological average seasonal and geographical variations in the NECC. It was found to have strong zonal variations in velocity and a rapid onset from weak westward flow in the (northern hemisphere) spring to an intense eastward flow during summer. Its flow is controlled by changes in the curl of the wind stress [*Garzoli and Katz*, 1983]. The rapid summer intensification of the NECC coincides with a simultaneous intensification of westward flow in the SEC and a deep-

Paper number 7C0182.
0148-0227/87/007C-0182$05.00

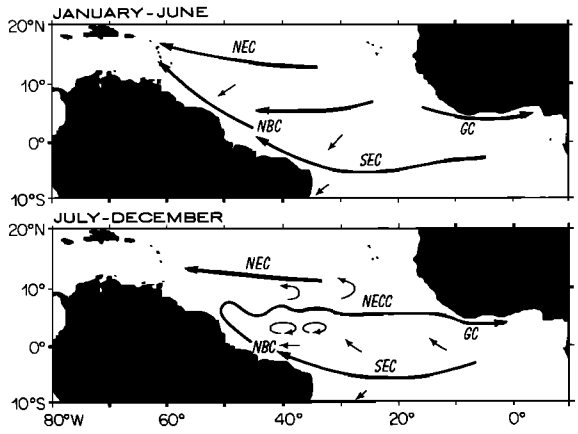

Fig. 1. Schematic diagram summarizing the main patterns observed in the SEQUAL and FOCAL drifter trajectories. NEC is the North Equatorial Current, NECC is the North Equatorial Countercurrent, SEC is the South Equatorial Current, NBC is the North Brazil Current, and GC is the Guinea Current.

ening of the thermocline near 3°N between these two currents. Thus the seasonal variation of the NECC is part of the whole interrelated equatorial response to the seasonal wind forcing.

This paper describes the currents in the upper ocean, focusing on the NECC. The organization is as follows: Section 2 discusses details of the drifting buoy and current meter measurement program and compares the two techniques where measurements overlap. Section 3 presents results of the drifter trajectories, concentrating on large-scale aspects of the circulation. Section 4 discusses zonal and meridional velocity profiles in the NECC from the drifters and vertical velocity profiles from moored current meters. The horizontal transport of the NECC and vertical transport out of the near-surface layer are estimated. Section 5 shows velocity time series in the NECC: a 23-year series constructed from historical ship drifts, a $2\frac{1}{2}$-year series from drifters, and a 20-month series from current meters. Interannual variations, seasonal variations, and higher frequencies are discussed. Section 6 examines more closely the higher frequencies associated with meanders, waves, and eddies in the NECC and SEC by using lagged space-time correlations. These fluctuations are found to be modulated seasonally. Similarities with numerical model predictions are presented. Section 7 summarizes the main points discussed in the paper.

2. Data

During 1983–1984 a single current meter mooring was placed near the center of the NECC near 6°N and 28°W to measure velocity time series at several depths. Thirty drifters were released along the NECC at several places and times to measure characteristic trajectories and the velocity structure. The complementary French Programme Français Océan et Climat dans l'Atlantique Equatorial (FOCAL) released 23 drifters in the SEC, a few of which reached the NECC [*Reverdin and McPhaden*, 1986]. The FOCAL drifters have been merged with SEQUAL's in this paper.

Drifting Buoys

The SEQUAL buoys were made by Polar Research Laboratory, Carpinteria, California. Twenty were TIROS oceanographic drifters (TODs), and six were mini TODs. All buoys measured sea surface temperature; 13 also measured wind speed by means of a Savonius rotor on the antenna housing. All TODs and one mini TOD had a 20-m^2 window shade drogue centered at a depth of 20-m. The tethers were configured to decouple the motion of the buoy from the drogue and to eliminate loss due to fish bite. Each tether consisted of a 50-m section of buoyant wire rope which floated near the sea surface and a 15-m section of wire rope that descended to the drogue. The remaining five mini TODs had a smaller drogue with area of 2.2 m^2 hung directly below the buoys and centered at a depth of 5 m.

The limited information that we have about the drogues and tethers suggests that at least the floating ones worked well and stayed attached for a long time. Two TOD buoys were retrieved at sea in the Gulf of Guinea on one of the SEQUAL cruises, thanks to the efforts of E. Katz. These two buoys and their tethers and drogues, which had been at sea for 217 days, were in excellent condition and were subsequently relaunched on a later cruise. The evidence from other TOD buoys picked up at sea by fishermen suggests that the drogues were attached when the buoys were found. However, we were not able to recover and inspect any of these drogues and tethers.

SEQUAL buoys were launched in the vicinity of the NECC on three SEQUAL and three FOCAL cruises. Seven buoys

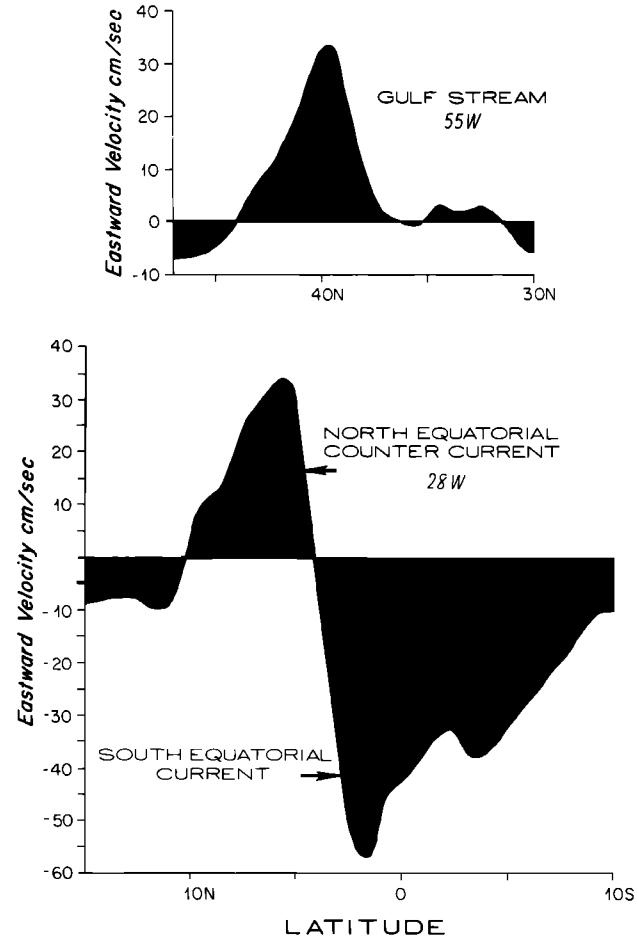

Fig. 2. Average yearly eastward surface velocity in the Gulf Stream near 55°W and average for July in the North Equatorial Countercurrent (NECC) and South Equatorial Current (SEC) near 28°W from historical ship drifts. Both sections are approximately 20° in longitude east of where the Gulf Stream and NECC leave the western boundary and have the swiftest currents. The amplitude and shape of the near-surface Gulf Stream and NECC are remarkably similar. Two major differences are the seasonal reversal of the NECC and the large shear between it and the South Equatorial Current.

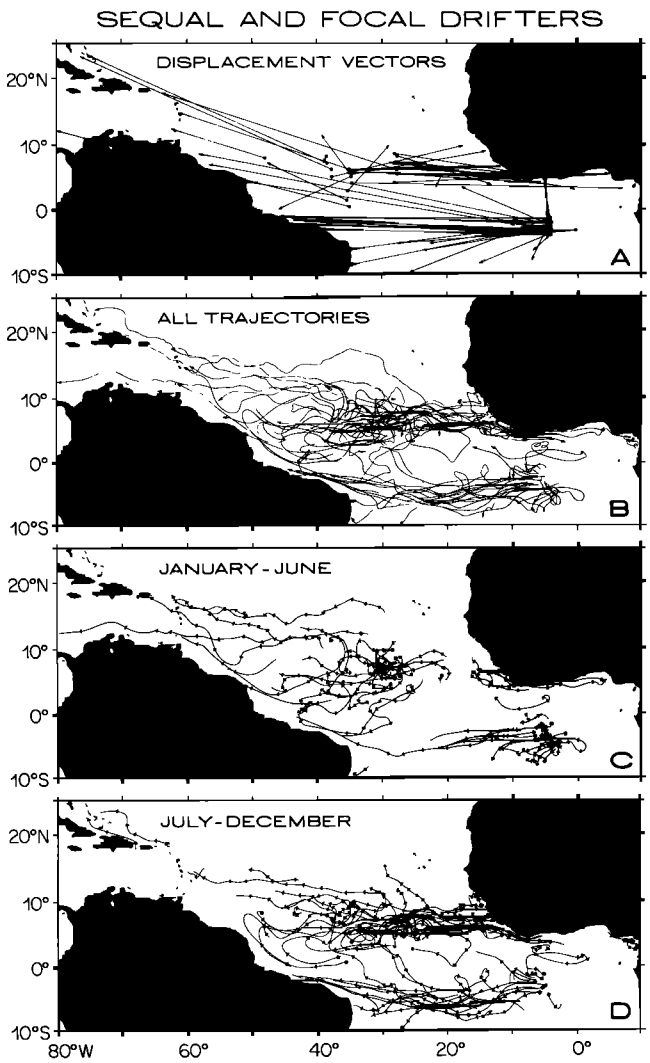

Fig. 3. Summary of drifting buoy trajectories. (*a*) Total displacement vectors from launch (dot) to final position (arrowhead) of SEQUAL drifters launched north of the equator and FOCAL drifters launched south of the equator. (*b*) All SEQUAL and FOCAL trajectories superimposed. Trajectories were smoothed with a 10-day filter to remove high-frequency oscillations. (*c*) Trajectories during spring (January through June) when the NECC disappears west of 20°W. Arrowheads are spaced at 10-day intervals. (*d*) Trajectories during fall (July through December) when the NECC flows eastward across the Atlantic into the Guinea Current.

were launched in February 1983 (five along 28°W, two along 20°W) to obtain characteristic springtime trajectories. Two were launched in April and three in July near 35°W to measure the startup of the NECC. Nine buoys were launched in the NECC in September (four along 38°W, five along 28°W). Three buoys that were recovered at sea were relaunched in March 1984 along 28°W as a second look at springtime trajectories, and a mooring beacon began its drift in April near 28°W. This satellite beacon, which was used to monitor the position of a current meter mooring, was knocked from the mooring when an unknown ship collided with it. Since its trajectory closely agreed with nearby drogued buoys, it was included in the analysis. The last five buoys (mini TODs) were launched in August 1984 along 35°W from 0° to 5°N in order to measure inflow from the SEC into the NECC and to obtain a second realization of the NECC. One additional recovered buoy was relaunched in November 1984 near 8°N, 48°W in the western NECC.

The SEQUAL drifting buoy data consist of 9800 buoy days of trajectories and velocities. The average lifetime of drifters was 316 days; the longest was 678 days. Seventeen buoys grounded (or were stolen close to shore): two on the Bahamas, five on the Antilles (Dominica, Grenada, Martinique, Saba, and Saint Lucia), one in Nicaragua, and nine on the coast of Africa (two in Liberia, two in Ghana, two in the Ivory Coast, one in Nigeria, one in Guinea, and one on São Tome). Three buoys were clearly stolen at sea, and we tracked two of the pirate vessels, one near Africa, the other near Brazil. Another buoy was very probably stolen, as its last transmitted temperature and position diverged from normal as if the buoy were out of the water and being transported by boat. Six buoys stopped transmitting off the coast of Africa where numerous fishing boats work.

Buoy positions were calculated from the Doppler shift of the transmitted signal as it was received by a passing TIROS-N/NOAA series satellite. These satellites have a near-polar, sun-synchronous orbit with a nominal altitude of 870 km and a period of 102 min. Tracking was by Service Argos at the Centre National d'Etudes Spatiales in Toulouse, France, On average, about six fixes were received per buoy per day. The precision of a fix of a satellite beacon on the roof of a building at Woods Hole Oceanographic Institution (WHOI), Woods Hole, Massachusetts, was estimated to be ± 0.3 km N-S and $\pm$ 0.4 km E-W (C. Collins, personal communications, 1983).

Erroneous data were eliminated by visually checking plots of the positions and velocity between positions and discarding obviously incorrect values. Four values per day of position, temperature, and wind speed were linearly interpolated at six-hour spacings. Values were smoothed with a 2-day Gaussian shaped filter ($\sigma = 0.5$ days) to reduce high-frequency oscillations and noise due to measurement errors. A cubic spline function was used to calculate velocity at the final positions. Trajectories and time series of wind speed, temperature, and u and v velocity components were plotted for each buoy. A more complete description of the buoys and plots of the data are given by *Richardson and Wooding* [1985]; results of the first year are discussed by *Richardson* [1984*a*].

Twenty-three FOCAL drifters, manufactured by CEIS Espace, Toulouse, France, were deployed in the SEC between June 1983 and July 1984. The buoys were equipped with a 20-m^2 window shade drogue centered at a depth of 15 m and connected to the buoys with a partially floating tether. A 117-m-long thermistor chain was attached to all but the last four buoys deployed.

FOCAL buoys were deployed in groups of four or five in June and November 1983 and February, May, and July 1984 along 4°W between 1°S and 4°S. Of the 23 buoys launched, five were retrieved at sea, four stopped transmitting at sea, one grounded in the Gulf of Guinea, and the rest grounded either on the Brazilian coast or shelf or further north on French Guyana, Surinam, and Guyana. The average buoy lifetime was about 166 days.

The FOCAL buoys were also tracked by Service Argos. Details of these buoys, deployments, and some specific results are given by *Reverdin and Kartavtseff* [1984], *Reverdin et al.* [1984], and *Reverdin and McPhaden* [1986].

Current Meter Mooring

Four vector-measuring current meters were deployed at depths from 20 to 300 m on a surface mooring near 6.1°N, 27.9°W in 4360 m of water. The mooring was kept in place for

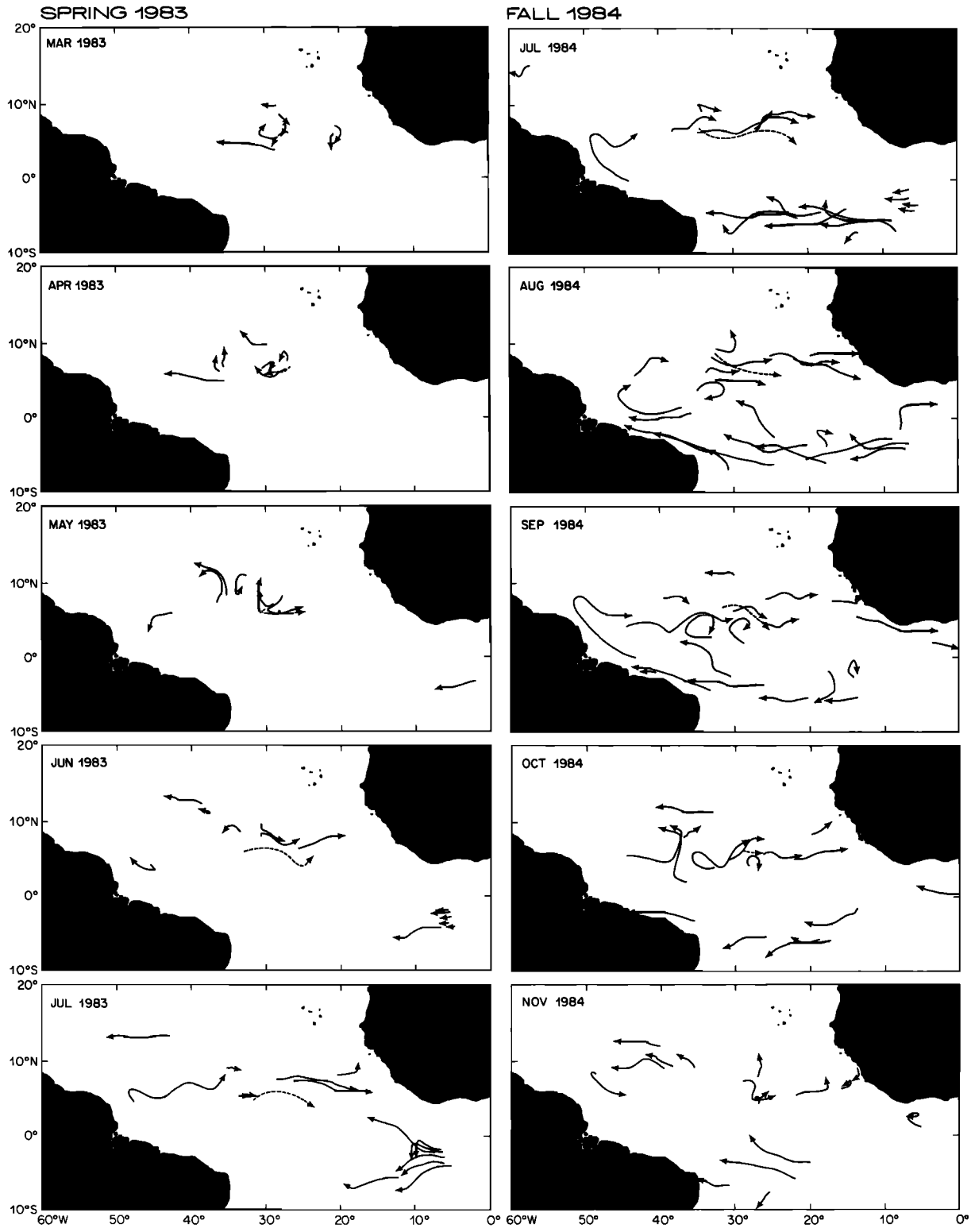

Fig. 4. Monthly composites of buoy trajectories smoothed with a 10-day filter. One set is from March to July 1983 showing spring trajectories. The second set is from July to November 1984 showing fall trajectories. In March to May 1983 one can see the gradual westward advection and mesoscale fluctuations located between 5° and 10°N. The startup of eastward flow in the NECC occurs in late May (one buoy) and during June and July. The fall 1984 trajectories show westward flow in the SEC, the retroflection of North Brazil Current into the NECC, waves and loops in the NECC, and the westward turning of buoys that moved from the NECC into NEC during late fall. December was the latest month that any buoy drifted eastward in the NECC.

6 months and was reset twice in the same location for a total of $19\frac{1}{2}$ months, from February 25, 1983, to October 12, 1984.

The current meters measured velocity and temperature over 15-min intervals. Values were smoothed with a 2-day Gaussian-shaped filter and were subsampled daily. Wind velocity at a height of 3 m above the surface, air temperature, sea surface temperature, solar radiation, and barometric pressure also were measured on the surface mooring. More infor-

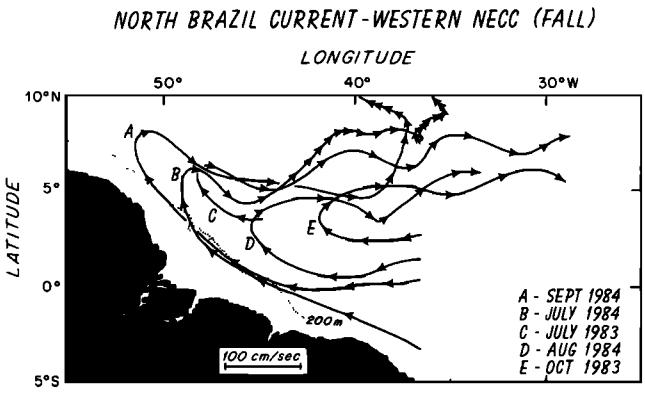

Fig. 5. Buoy trajectories showing the retroflection of the North Brazil Current into the western NECC during fall. No buoys continued up the coast past the NECC during fall. Arrows are spaced at 5 days.

mation about the instruments and data are presented by *Levy and Richardson* [1985], *Richardson* [1984*b*], and *Payne* [1984].

Buoy–Current Meter Comparison

Five buoys drifted within 30 km of the mooring, two of these within 5 km. A comparison of velocity from these buoys and the current meter (at 20-m depth) shows good agreement that in general is best for closest passes. No systematic difference is seen when buoy velocities are plotted against current meter velocities. The root-mean-square difference in velocity components between 23 pairs of simultaneous drifter–current meter measurements at less than 30-km separations is 5.9 cm/s. This is about the same as between pairs of drifter measurements at equivalently close passes (6.8 cm/s). The scatter seems to be due primarily to spatial gradients in velocity associated with energetic 4- to 5-day near-inertial oscillations plus large-scale horizontal shear in the NECC. Part of the scatter between the drifters and the current meter could also be due to the force of wind and waves on the buoy and to vertical shear in the upper 30 m of the water column.

Three of the close buoy–current meter passes (nine daily velocity observations) were made while wind velocity was being measured at the mooring. Comparing wind velocity with the difference between buoy and current meter velocities revealed that the buoys had an average downwind velocity (and standard error) relative to the current meter velocity of 3.8 cm/s ($\pm$0.9 cm/s), or 0.59% of the wind speed. The cross-wind velocity was much smaller than this, 0.4 cm/s ($\pm$0.8 cm/s).

Ship Drifts

Historical ship drifts were obtained from the U.S. Naval Oceanographic Office, Bay Saint Louis, Mississippi. They consist of approximately 438,000 individual observations within the region bounded by 20°S–20°N, 10°E–70°W, and the coasts of Africa and South America. Further information about these data can be found in the work of *Richardson and McKee* [1984] and *Richardson and Walsh* [1986].

3. Buoy Trajectories

General Pattern

Figure 1 shows a schematic interpretation of the trajectories. Figure 3 is a summary of the trajectories, showing overall displacements, superposition of all trajectories, and a subdivision of trajectories into two half-year time periods: spring (January–June) and fall (July–December), the seasons when the NECC disappears and appears. Figure 4, monthly composites, shows some details of the trajectories. Most buoys drifted westward except for those in the Guinea Current, those in the NECC during fall, and a few near the equator that drifted eastward.

South Equatorial Current and North Brazil Current

South of the equator, most buoys in the SEC drifted westward into the North Brazil Current and grounded on the coast of Brazil east of the Amazon owing to an onshore component of velocity. They typically required 5 months to make the trip from 4°W to 45°W, although the time varied widely for different deployments. As they drifted westward from 10°W to 25°W, they moved south owing to meridional surface divergence near the equator. West of 25°W they turned northward and accelerated as they approached Brazil. The swiftest buoys of the whole equatorial region, with speeds of up to 167 cm/s, were in the North Brazil Current near the equator. Among 11 buoys released by *Molinari* [1983] from 7° to 11°S and from 23° to 31°W, those north of 8°S also tended to drift northwestward, and those south of 8°S drifted southwestward.

The northwestward component of drift along the coast shows that the North Brazil Current flows continuously northward across the equator throughout the year. During spring the North Brazil Current continues up the coast into the Guyana Current and into the Caribbean. During fall the North Brazil Current retroflects, or veers offshore, between 5° and 10°N and flows eastward, forming the western limb of the NECC. Evidence from five trajectories in the west is that virtually all the North Brazil Current water turns eastward into the NECC during fall (Figure 5). The retroflection matches subsurface observations of a large stationary eddy [*Bruce et al.*, 1985].

The drifts from a few buoys in the mid-Atlantic suggest that cross-equatorial flow varies seasonally (Figure 3). Five buoys in the SEC moved northward across the equator during fall; three of these entered the NECC for various lengths of time. Two buoys moved southward across the equator (near 30°W) in spring and entered the North Brazil Current. One SEC buoy drifted southward into the Brazil Current.

Two buoys near the equator, one near 30°W in mid-March 1984 and another near 40°W in early May 1984, drifted eastward as part of the reversal which occurs in the western SEC near the equator in spring. The two periods of eastward current match perfectly two periods of eastward wind velocity at Saint Peter and Saint Paul rocks, located near 1°N, 29°W [*Colin and Garzoli*, 1987]. This reversal is generated as the intertropical convergence zone moves north across the equator, the trade winds relax there, and the eastward pressure gradient drives an eastward near-surface velocity [*Katz et al.*, 1981]. Two other buoys near the equator and 5°W drifted eastward in January and February 1984, when winds were northeastward.

North Equatorial Countercurrent

Buoys in the NECC drifted eastward during fall in the band 4°–10°N approximately. About half continued eastward into the Guinea Current and Gulf of Guinea, and about half drifted northward into the North Equatorial Current (NEC) and turned westward. A few buoys hovered near the coast of

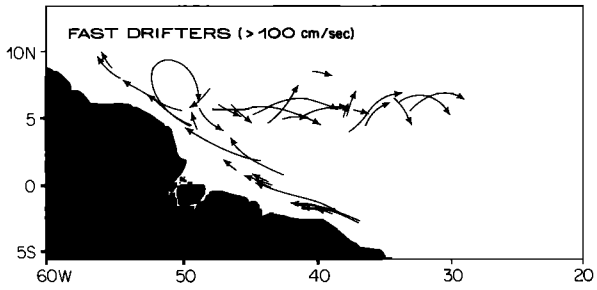

Fig. 6. Segments of trajectories of buoys that drifted faster than 100 cm/s after being smoothed with a 10-day filter to suppress inertial oscillations. Fastest speeds (2-day smoothing) were 167 cm/s in the North Brazil Current near the equator and 143 cm/s in the western NECC.

Africa near 15°W, and a few others were short-lived. Many buoys that entered the NEC seemed to have been left behind by the NECC as its northern edge moved south during late fall.

The buoys suggest that the inflow to the NECC occurs from the North Brazil Current retroflection and from the western SEC. Although all North Brazil Current buoys retroflected into the NECC during fall, one drifted northward out of it after a month and into the NEC. Several retroflected buoys dipped south a few hundred kilometers near 45°W and meandered eastward. A few buoys became temporarily trapped in clockwise loops centered between the western NECC and SEC. Both the meanders and clockwise loops are shown schematically in Figure 1. Buoys in this western region drifted very fast, with speeds of up to 143 cm/s (Figure 6). One of the few buoys to cross the Atlantic in the NECC took 5 months to do it (Figure 7). Most others started in the wrong place, were too

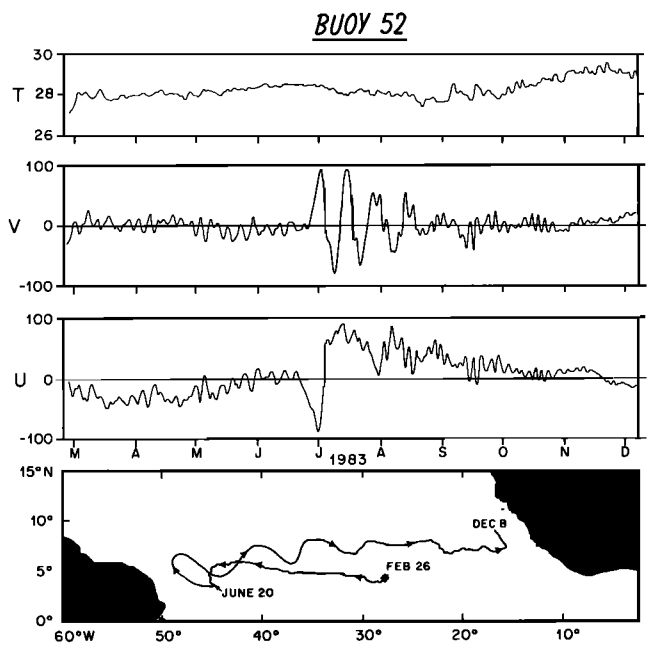

Fig. 7. Trajectory of buoy 52 from February 26 to December 8, 1983. The time series and trajectory were smoothed with a 2-day filter. The Lagrangian period and wavelength of the meanders is approximately 15 days and 700 km, and the latitudinal displacement is 300 km in the west. Higher-frequency oscillations are 4- to 5-day near-inertial waves which have amplitudes here of up to about 20 cm/s.

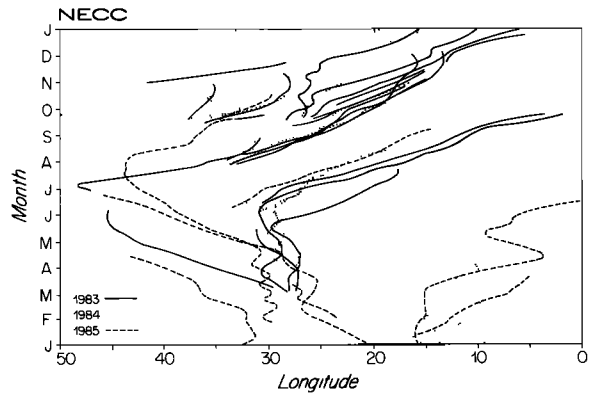

Fig. 8. Time-longitude plot of buoys in vicinity of the NECC. The latitude limits of buoys are 4°–9N, shifting south to 3°–6N east of 10°W to follow the Guinea Current. Eastward velocity is indicated by the direction and slope of the trajectories. The most nearly horizontal ones are the swiftest. During January–June the buoys gradually drift westward and oscillate zonally with periods of approximately 3–6 weeks. In late May to June, usually, the buoys switch direction and drift eastward. Eastward flow continues through the end of the year with the exception of a few brief reversals shown by buoys that looped near the NECC-SEC boundary (near 35°W in October 1984) or in strong eddy motion in the NECC (near 28°W in November 1984 and near 25°W in September and October 1983).

late or too slow to make it across, or were sidetracked into the SEC or NEC.

Spring trajectories show that west of 18°W the NECC disappeared and that where it had been located, buoys drifted generally westward into the North Brazil Current and up the coast (Figure 3). A region of zonal divergence is seen between these westward drifting buoys and the eastern buoys off Africa and in the Guinea Current. A few anomalous buoys drifted eastward in the midst of the westward trend. Some of these were in the NECC as it started up in late May and June, and four were near the equator, as was mentioned above.

Figure 8, a time-longitude plot of trajectories located between 4° and 9°N, shows the seasonal reversal of the NECC. The general trend of eastward flow during fall and westward during spring can be seen, as can the NECC–Guinea Current connection. The trajectory and velocity from one buoy clearly illustrates several aspects of the seasonal variation (Figure 7). This buoy drifted westward near 5°N during March–June, accelerated northwestward in June, retroflected into the NECC during July, and meandered eastward during July–November. At the end of its trajectory in early December, it looked as if it was about to enter the NEC and drift westward, as other buoys did. Two other buoys drifted long distances back and forth in the NECC region for 2 years, but their trajectories are more complicated than this one.

North Equatorial Current

Buoys that entered the NEC drifted west-northwestward toward the Antilles with a very steady flow of about 22 cm/s (Table 1). Spring and fall trajectories look similar. The characteristic travel time from 30°W to 60°W was about 5 months. One significant departure from this general pattern is a buoy that stalled near 15°N, 51°W for a month in the vicinity of some seamounts, the shallowest of which is about 700 m from the surface. Of the nine buoys that reached the Antilles (two of which arrived in the Guyana Current) three were picked up by fishermen and returned, two grounded or were stolen, one

TABLE 1. Average Velocity and Variance of Currents, Determined From Drifting Buoys

Current*	Number of Observations	Box Limits†	Average Velocity, cm/s		Variance, cm²/s²		EKE, cm²/s²
			$\bar{u}$	$\bar{v}$	u'^2	v'^2	
NEC	2977	10°–18°N, 40°–60°W	−21.8	2.9	143	161	152
WNECC (fall)	217	5°–8°N, 40°–50°W	41.0	−4.6	2568	2226	2397
WNECC (spring)	144	5°–8°N, 40°–50°W	−23.2	−3.8	131	117	124
ENECC (fall)	1590	5°–8°N, 25°–30°W	21.5	3.1	376	460	418
ENECC (spring)	1604	5°–8°N, 25°–30°W	−3.2	−1.5	280	171	226
NBC	1158	4°S–3°N, 35°–48°W	−56.3	12.6	1176	454	815
GC	583	3°–6°N, 5°E–5°W	33.0	1.0	928	319	624
SEC	5553	2°–8°S, 10°–30°W	−27.3	−1.8	273	167	220

*WNECC is the western NECC, ENECC is the eastern NECC, GC is the Guinea Current, and NBC is the North Brazil Current.

†Individual velocity observations were grouped into boxes, and average values were calculated using all available data.

drifted north of the islands, and three passed through the islands. One of these three drifted through the southern Caribbean and grounded on Nicaragua, one cut through the northeastern edge of the Caribbean, and one skirted through the northeastern islands. These later two subsequently grounded on the Bahamas. The evidence from drifters thus is that most water which enters the NEC from the NECC flows into the Caribbean, presumably to continue westward then northward and to emerge in the Gulf Stream.

Guinea Current

The Guinea Current flows eastward in both seasons. During fall a direct connection between the NECC and the Guinea Current can be seen in the buoy trajectories. In spring east of 18°W the buoys that had been in the NECC continue into the Guinea Current. Buoys accelerated after entering the Gulf of Guinea and reached peak eastward velocity of approximately 100 cm/s near 5°W.

One buoy looped between the Guinea Current and SEC, implying that water is exchanged between these two currents. Another Guinea Current buoy reversed its direction for a month during April and May 1985 and then continued eastward again. One buoy drifted into the northeastern corner of the Gulf of Guinea and stayed there for 7 months, implying the existence of a convergence region there, as a few other drifters have done [*Piton and Fusey*, 1982].

Discussion of Trajectories

The general features described above have all, with one major exception, been observed with historical ship drifts. What is new is the collection of trajectories that give estimates of the characteristic paths and velocities of water parcels and a detailed measure of space-time variability. The major new finding is the buoys' evidence of complete retroflection of the North Brazil Current into the NECC during fall. Ship drifts suggested that a portion of the North Brazil Current continued up the coast into the Guyana Current during fall. There is, however, the possibility of some continuous northward flow on the shelf inshore of the buoy trajectories (Figure 5).

We should be cautious about interpreting patterns from trajectories because only a small number of buoys were launched and in only a few spots. Regions of surface convergence (NECC) tend to trap the buoys and regions of divergence (equator) repel the buoys, distorting the large-scale patterns.

The drifter trajectories are consistent with, and help interpret, satellite images from the coastal zone color scanner and maps of sea surface salinity. Fall images show a plume of water originating near the mouth of the Amazon and following the left edge of the North Brazil Current around the retroflection and along the northern edge of the NECC [*Muller-Karger et al.*, 1986]. A clear discontinuity between the North Brazil Current and the Guyana Current is observed. Composite maps of surface salinity for fall show a low-salinity tongue emanating from the Amazon and also following the left edge of the North Brazil Current into the northern NECC [*Perlroth*, 1966; *Neumann*, 1969]. Spring images and salinity maps show that the Amazon water flows northward parallel to the coast.

The trajectories are also consistent with model simulations by *Philander and Pacanowski* [1986*a*] that show the North Brazil Current continuing up the coast in winter and spring but veering offshore into the NECC during summer and fall. This causes the model heat flux to have a huge seasonal variation; in January the northward heat flux reaches 1.8×10^{15} W across 8°N, but in July it drops to -0.2×10^{15} W. There is the possibility that the large-scale thermohaline circulation in the Atlantic and the near-surface equatorial response to wind forcing are tightly linked in vicinity of the NECC.

Buoys in the NECC tended to remain within the same latitude band and slow as they drifted eastward. These plus historical ship drifts indicate a near-surface convergence of warm water (both meridionally and zonally) in the NECC and an implied downwelling. The transport of downwelled water out of the upper layer was estimated from ship drifts to be 8×10^6 m³/s (ship drifts were used because of the larger data set). To obtain this value, the annual average surface convergence was calculated between 3° and 8°N west of 10°W and multiplied by an assumed mixed layer depth of 30 m. The meridional convergence of velocity between 3°N and 8°N was estimated to be 8.5 cm/s from the mid-Atlantic track line lying near 28°W. Multiplying this value by an assumed 30-m depth and the 30° longitude width of the Atlantic also gives an estimated transport out of the near-surface layer of 8×10^6 m³/s. This suggests that most downwelling is due to the meridional variation of velocity. The meridional convergence along 28°W between 3°N and 8°N has a seasonal cycle with an amplitude of around 4 cm/s; maximum values of ~12 cm/s occur during May–August. Model simulations by *Philander and Pacanowski* [1986*b*] show that most of the water that leaves the NECC

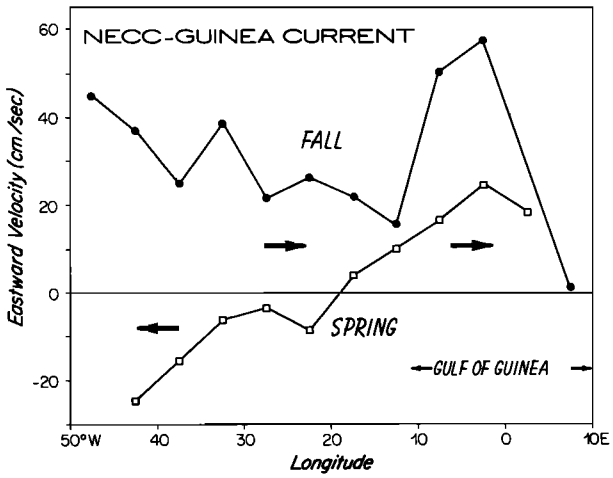

Fig. 9. Eastward velocity along the axis of the NECC–Guinea Current in fall (July–November) and spring (January–May). Average velocity values were calculated by grouping individual drifter observations into boxes 3° in latitude by 5° in longitude lying along the band 5°–8°N from 15° to 50°W and then dipping southward to 3°–6°N and eastward into the Gulf of Guinea. Values in boxes with fewer than 130 observations were omitted.

from the surface layer downwells; they give 10×10^6 m^3/s for the annual average downwelled transport. In their model the downwelled water flows equatorward and upwells north of the equatorial undercurrent, into the SEC to sustain near-surface divergent drift. The drifter, ship drift, and current meter results are consistent with this three-dimensional picture.

4. Velocity Profiles

Zonal Profiles

Average velocity was calculated along the mean position of the NECC (5°–8°N) and Guinea Current for two time periods: fall, when the NECC was swift, and spring, when the NECC disappeared (Figure 9). In fall the highest eastward velocity in the NECC, 45 cm/s, occurs in the far west, between 45° and 50°W. Velocity decreases to 15 cm/s between 10° and 15°W and then increases again to a peak of 57 cm/s in the Guinea Current between 0° and 5°W. The spring profile shows the reversal of the NECC; west of about 20°W, velocity is westward, increasing to a maximum of 25 cm/s between 40° and 45°W. East of 20°W, velocity is eastward, increasing to a peak of 24 cm/s in the Gulf of Guinea between 0° and 5°W. The spring velocity in the Gulf of Guinea includes the only buoy that reversed direction there (for a month and close to the coast), decreasing the average eastward velocity.

Vertical Profiles

Vertical profiles of velocity in the NECC were obtained by averaging time series at the current meter mooring location near 6°N, 28°W (Figure 10). The 1984 July–August profile of eastward velocity is 40 cm/s near the surface, decreasing to about 10 cm/s at 300 m. This implies that the NECC extends to an overall depth of about 350 m. The 1983 July–August profile has the same shape in the upper 150 m but is about 8 cm/s slower.

March–April profiles indicate weak (<4 cm/s) westward velocity below 20 m. At 20 m the velocity was 8 cm/s westward in 1983 and 8 cm/s eastward in 1984. Based on the visual correlation between velocity series at 20 m, 50 m, and 75 m, the 50-m and 75-m records would also have been eastward during March–April 1984 had they been measured in 1984. The estimated standard error for March–April, ~ 10 cm/s at 20 m, indicates that the velocities are statistically indistinguishable from zero. It appears that at this site the subsurface NECC vanishes in spring (March–April), as does the surface NECC.

Little seasonal variation is seen in the northward velocity component. Averages over large portions of the records indicate that a mean equatorward flow of about 6 cm/s is centered near a depth of 50 m. The records are too short for much statistical confidence considering the large-amplitude variations in the time series; the standard error at 50 m is estimated to be 3 cm/s, suggesting that the mean is not statis-

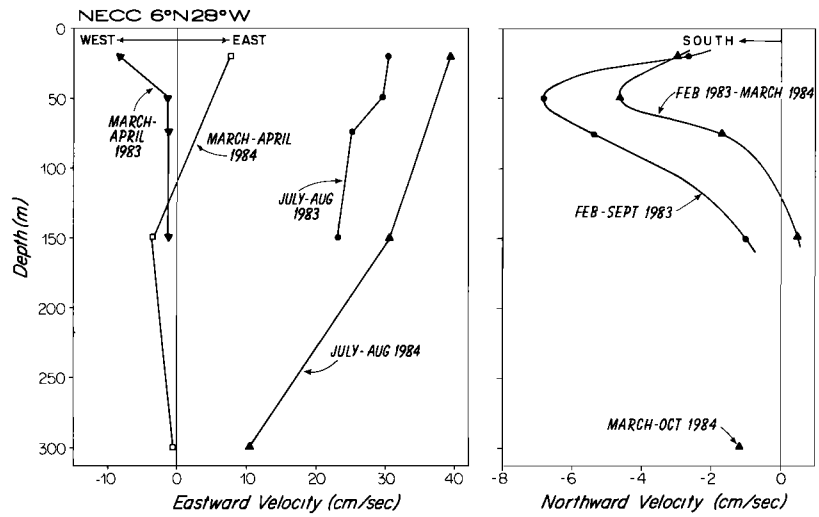

Fig. 10. Vertical profiles of velocity obtained from the current meter mooring at 6°N, 28°W (see Figure 16). The July–August profiles were chosen to match the time of maximum eastward subsurface velocity. The March–April profiles match times of minimum eastward velocity. The 300-m 1984 value is an average over April. The standard error in u at 20 m is estimated to be approximately 13 cm/s for these short pieces of the records. Profiles of northward velocity were averaged over longer time series because little seasonal variation was seen in the records. The standard error in v at 50 m is estimated to be approximately 3 cm/s.

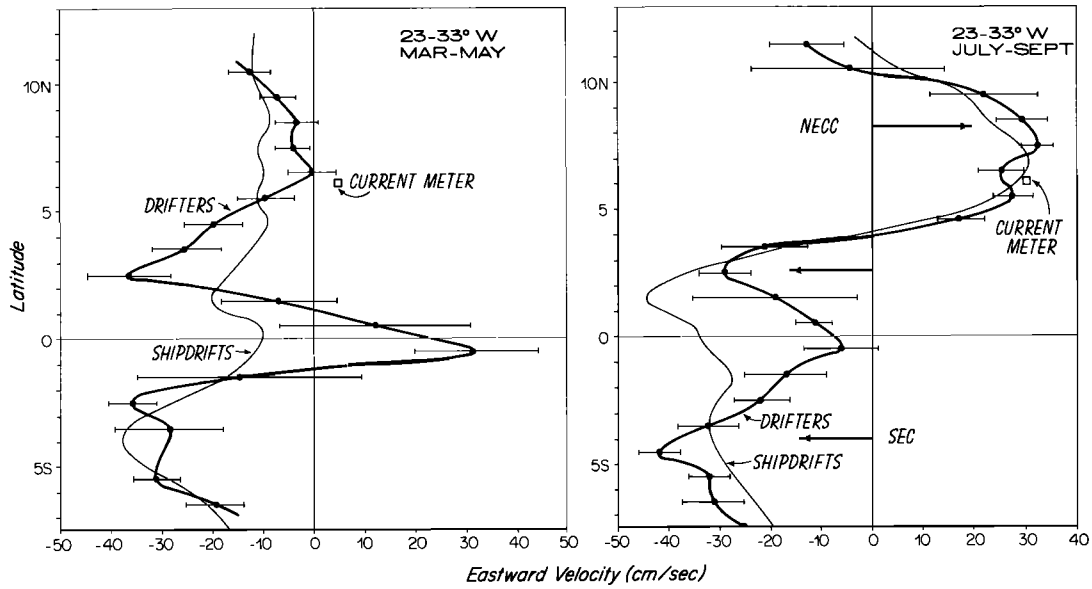

Fig. 11. Meridional profiles of eastward velocity across the NECC in fall (July–September) and spring (March–May) using data from 1983–1985. Individual buoy velocity values were grouped into 1° latitude by 10° longitude boxes in the central Atlantic between 23–33°W. Average values over the same months from the 20-m current meter at 6°N, 28°W, and historical ship drifts are added. Error bars indicate estimates of standard errors. The densest data are located from 5°N to 10°N in the NECC and from 3°S to 8°S in the SEC. Between these areas there are very few trajectories, and the profiles are probably not a good indication of long-term averages.

tically different from zero at the 95% confidence level. However, the trend of equatorward flow is consistent in averages made over the first 6 months and over the whole 12 months. Assuming a uniform equatorward velocity over a 30° longitude band across the Atlantic yields an equatorward transport between 10- and 150-m depth of 19×10^6 m^3/s for the 6-month average and 9×10^6 m^3/s for the yearlong average. These are consistent with the estimated transport downwelled from the surface NECC.

Meridional Profiles

NECC. Meridional profiles of velocity were calculated by grouping all possible buoys into boxes 1° in latitude. In the mid-Atlantic from 23° to 33°W, the NECC is located between 4° and 10°N and has a peak speed of 33 cm/s at 7.5°N (Figure 11). Individual profiles from 1983 and 1984 (not shown) agree closely with this average, as do the profile from ship drifts and the current-meter value.

Spring profiles at 23°–33°W show weak westward current, with a minimum velocity close to zero, at 6.5°N. The current meter measured an eastward velocity of 5 cm/s during spring. This difference could be due to different data sets, different averaging schemes, large standard errors associated with each average, or the downwind component of drifter velocity relative to current meter velocity, noted earlier. The buoy profile differs considerably from ship drifts, which suggests westward velocity of 10 cm/s throughout the NECC region, a difference of about 5 cm/s.

The Pacific NECC has a similar profile (between 100° and 130°W) but a slightly higher mean velocity, ~50 cm/s [*Hansen and Paul*, 1984]. Although the Pacific NECC slows in spring, it does not reverse direction [*Patzert and McNally*, 1981].

The eastward volume transport of the NECC was estimated to be 54×10^6 m^3/s by combining the meridional profile of velocities from drifters (Figure 11) and the vertical profile of velocity from current meters averaged over July and August 1984 (Figure 10). The meridional profile was offset at different depths to make it agree with the vertical profile at 6°N, and the transport was summed over latitude and depth. A major assumption was that the meridional structure of subsurface flow is the same as that at the surface. If the deep NECC is in reality much narrower than the surface flow, then the real transport would be less. Large fluctuations in integrated transport per unit width occur on short time scales at the mooring, casting further uncertainty on the estimate.

Earlier estimates of transport are generally much smaller than those given here. *Bubnov and Egorikhin* [1979] found 18×10^6 m^3/s during June–September 1974 at 23.5°W, using moored current meters and profilers. *Cochrane et al.* [1979] give a value for the NECC near 33°W, in August, of 35×10^6 m^3/s. *Philander and Pacanowski* [1986*b*] report that the simulated NECC of their model at 30°W persists throughout the year below the surface, with a maximum transport of 17×10^6 m^3/s in July–August and a minimum of 3×10^6 m^3/s in March–April.

SEC. Meridional profiles indicate two maxima in the westward flowing SEC, one with velocity between 30 and 44 cm/s centered near 2°N and the second with velocity between 36 and 42 cm/s centered near 3°–4°S. The maxima are separated by a minimum located at 0.5°S with velocities ranging from 6 cm/s westward (fall) to 32 cm/s eastward (spring). Although the number of buoys near the equator was quite small, and thus we would not expect the profiles to agree with ship drift climatology, the trend of near-zero or eastward velocity between 0° and 1°S seems clear from buoys, and it agrees with low average velocity measured with moored current meters near the equator [*Weisberg*, 1984*a*]. The historical ship drifts also show a minimum in velocity near the equator though it is much less pronounced. This is probably due to the few

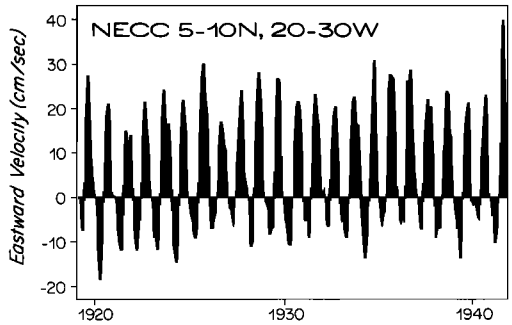

Fig. 12. Time series of eastward velocity in the NECC from historical ship drifts during the years 1919–1941, when the data were most numerous in time. Monthly average values were calculated by grouping individual observations in a box which extended from 5° to 10°N and from 20° to 33°W. On average, each velocity was based on 21 individual observations. Some months (December, June, July) of some years (1919–1934) were devoid of any observations, and these gaps were linearly interpolated. The series was smoothed slightly with weights of $\frac{1}{4}, \frac{1}{2}, \frac{1}{4}$ to reduce month-to-month noise.

hundred kilometer spatial averaging of each ship drift velocity. This minimum separating the SEC into two jets is an indication of the eastward flowing Equatorial Undercurrent.

In the southern SEC, where buoy data are most numerous, the agreement between ship drifts and drifting buoys is quite good, as was discussed by *Reverdin and McPhaden* [1986]. The major difference is a 6 cm/s slower speed of average ship drift velocity (between 3°S and 8°S). This could be due to interannual variations, since most of the buoy data come from 1984. A meridional profile across the equatorial Pacific between 110° and 130°W during fall 1979 from drifters is very similar in shape to the Atlantic profiles [*Hansen and Paul*, 1984]. The main difference is a slightly faster mean speed in the Pacific current jet, near 2°N.

5. Velocity Time Series

Three sources of long-term velocity time series exist for the NECC: historical ship drifts during 1919–1941, years when the number of observations peaked; drifting buoys during 1983–1985; and current meters during 1983–1984. The following discussion deals first with low-frequency, interannual variations, and then with higher frequencies.

The low frequencies were studied by grouping buoy and ship drift data into monthly space-time boxes spanning the NECC near the mooring at 28°W. The main finding is the extreme regularity of the seasonal cycle of eastward velocity seen in the space-time averages; very little interannual variability is detected. The current meter series shows the complicated variability that occurs at a single point and what appear to be differences in the 1983 and 1984 velocity fields: in 1984, eastward velocity was higher by about 10 cm/s. However, it is difficult to say much statistically about interannual variations with only a $1\frac{1}{2}$-year-long record.

Ship Drifts

A 23-year time series of velocity in the NECC was constructed by subdividing ship drifts into monthly averages for the years 1919–1941 (Figure 12). This long series demonstrates the extreme regularity in amplitude and phase of the NECC. Every year it peaks in summer and reverses in the spring. To estimate interannual variations consisting of variations of (1) the yearly mean, (2) amplitude of the seasonal cycle, and (3) its timing, an annual harmonic was fitted to values for each year. The average yearly eastward velocity (and standard deviation) was 5.3 cm/s ($\pm$2.2 cm/s), the average amplitude was 15.6 cm/s ($\pm$3.2 cm/s), and the average peak eastward velocity occurred on year day 256 ($\pm$12 days).

A kinetic energy spectrum calculated for the 23-year NECC series is shown in Figure 13. Of the total eddy kinetic energy (107 cm^2/s^2), 80% was in the zonal component, most of it centered near an annual period. In the eastward component, 68% of energy (58 cm^2/s^2) was in the band from 11.0 to 13.2 months. This is much larger than the energy in (eastward) variations at periods greater than 13 months, estimated to be 2 cm^2/s^2.

As measured by ship drifts, the western NECC has a larger amplitude of seasonal variation ($\sim$23 cm/s), but there are fewer observations, and the series is noisier. A search of other areas in the tropical Atlantic shows that only the SEC has as large a seasonal cycle as the NECC [see *Richardson and Walsh*, 1986]. However, the SEC has a much larger semiannual harmonic and larger year-to-year variations. The NECC thus emerges as having the largest and most regular seasonal cycle in the Atlantic.

Drifting Buoys

Time series of monthly eastward velocity are shown in Figures 14 and 15, and the average seasonal variation from ship drift climatology is added in Figure 15. Drifting buoys measured a very regular seasonal cycle, with westward velocity of about 6 cm/s in January through April, an onset of NECC in

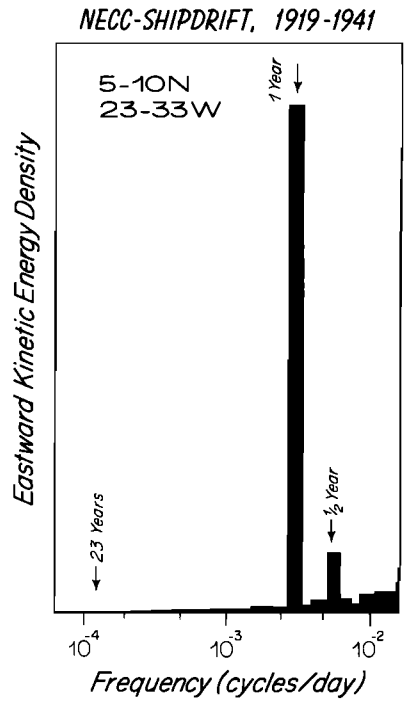

Fig. 13. Kinetic energy spectrum calculated using the 23-year ship drift time series consisting of monthly average eastward velocity in the NECC (5°–10N, 20°–33W). The spectrum is shown in energy-preserving form; the contribution of each frequency band is in proportion to the area under the curve in each band. The highest peak coincides with the annual harmonic, the second highest with the semiannual harmonic. The total eddy kinetic energy is 107 cm^2/s^2, of which 80% is in the eastward velocity component. The spectrum of northward velocity resembles the eastward except that the peaks at annual and semiannual periods are much lower.

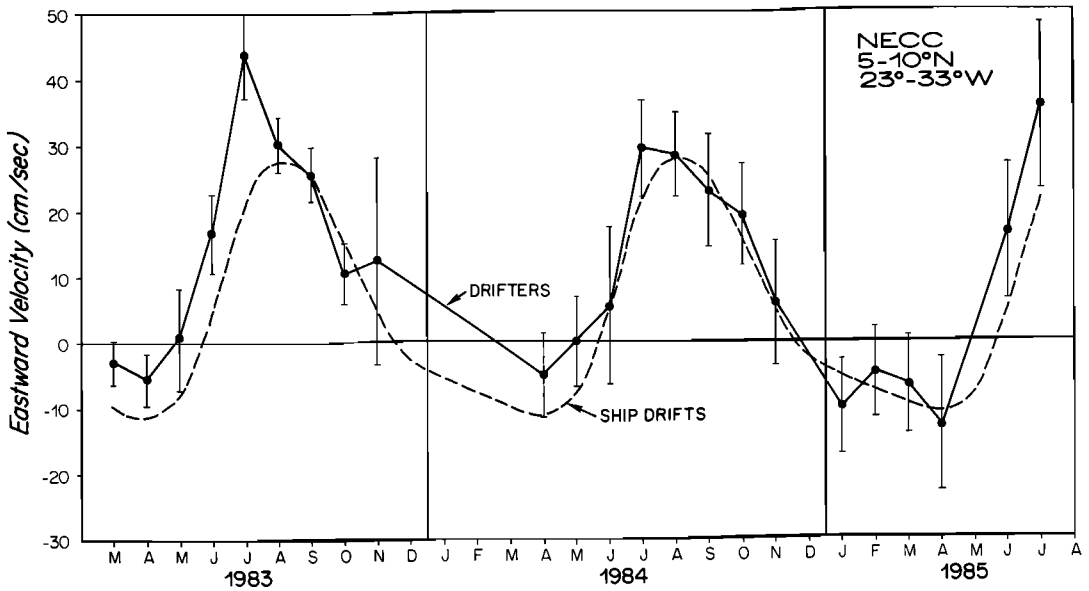

Fig. 14. Time series over 2½ years of eastward velocity in the NECC. Average seasonal variation from historical ship drifts during 1875–1976 is included. Individual drifter and ship drift velocities were grouped into monthly averages in a box which extended from 5° to 10°N and from 23° to 33°W. Values from months with fewer than 40 observations were omitted. Error bars indicate estimated standard errors.

May, a peak eastward velocity of about 35 cm/s in July, and a gradual decay during August–December. Each of the 3 years follows this pattern quite closely. Some yearly differences occur, such as June–July, which have a faster eastward velocity by about 12 cm/s in 1983 than in 1984, and March–April, which have faster westward velocity by 5 cm/s in 1985 than in 1983. However, the numbers of buoys in each month's average is small, and both higher-frequency oscillations and spatial gradients of velocity within the box could easily cause the observed differences. We conclude that interannual variations in velocity are masked in these drifter velocities by other sources of variability.

The seasonal time series from buoys and ship drifts are very similar in the overall shape and amplitude of the curves (Figure 15). The main difference is from March through July, when the ship drifts have greater westward velocity. Part of this discrepancy seems to be due to the concentration of drifters near the center of the NECC. When smaller boxes near the center of the NECC are used, the ship drift–measured onset of the NECC is earlier and faster, the peak velocity occurs in July, and the velocities in June and July agree much more closely with the drifter velocities. However, the discrepancy in March–May still exists, as we saw in the meridional profiles (Figure 11). Another part of the discrepancy could be due to shear between the upper few meters of water, where the ship's hull is located, and 20 m, where most of the buoys' drogues are centered. The January–April 1985 buoy values, which agree better with ship drifts, are primarily the mini TODs with smaller, shallower drogues. Part of the discrepancy could also be due to the force of wind and waves on the ships' hulls. The maximum climatological westward wind stress occurs in the NECC from December through April, which matches a portion of the time of the discrepancy. Thus although there are some nagging differences between ship drift and drifter time series, these differences are generally small and the two series agree well where the data are numerous.

Current Meters

Velocity time series from the current meters moored at 6°N, 28°W are shown in Figures 16 and 17, a superposition of 1983 and 1984 eastward series at 20 m is given in Figure 18, and spectra are shown in Figure 19.

Eastward velocity. The 20-m series shows very weak mean flow in February–April, a rapid onset of the NECC in May, and maxima in June of 60 cm/s in 1983 and 74 cm/s in 1984. From May through December the current continues to flow swiftly eastward with large-amplitude fluctuations. Although the onset of the NECC was very similar in 1983 and 1984 (Figure 18), the mean flows of the overlapping segments were noticeably different for the 2 years; the average of 1984 has a

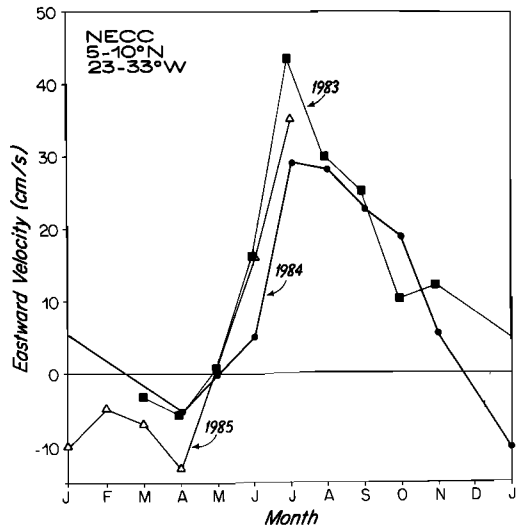

Fig. 15. Superposition of the NECC time series. The year-to-year differences are smaller than the standard errors. Some of these differences could be caused by a particular grouping of drifters within the box and the presence of energetic high-frequency oscillations.

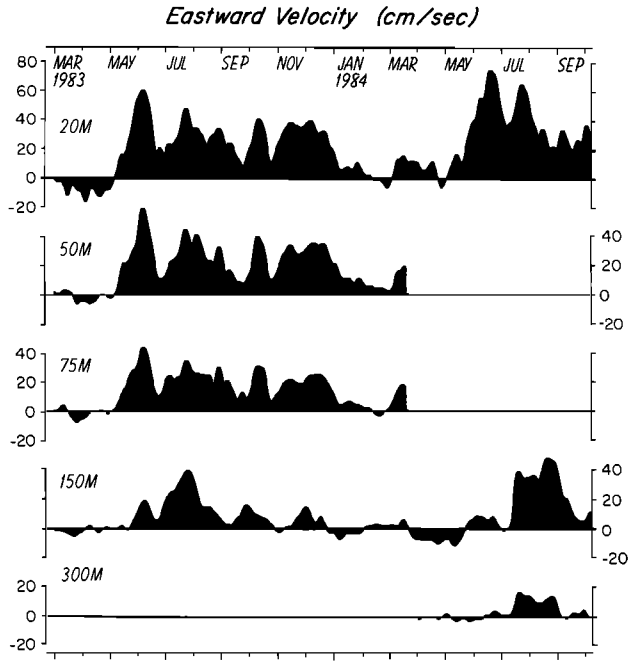

Fig. 16. Eastward velocity time series from the current meters moored near the center of the NECC at 6°N, 28°W. The series were smoothed with a 10-day Gaussian filter to reduce high-frequency oscillations.

larger velocity by 10 cm/s. However, the difference was not statistically different from zero at the $\alpha = 0.05$ level of significance, and the buoy velocity series (Figure 15) suggest that 1983 had greater velocity in the NECC than 1984.

The 20-m, 50-m, and 75-m records have high visual correlation and similar amplitudes in both u and v components. The correlation is weaker between 20- and 150- or 300-m records, and the amplitudes are smaller at depth. What stands out is the seasonal cycle in eastward velocity, which extends down to 300 m. Eastward velocity occurs below 100 m in July and August, with peak speeds of 48 cm/s at 150 m and 18 cm/s at 300 m; near-zero (average) velocity occurs during January–May at these depths.

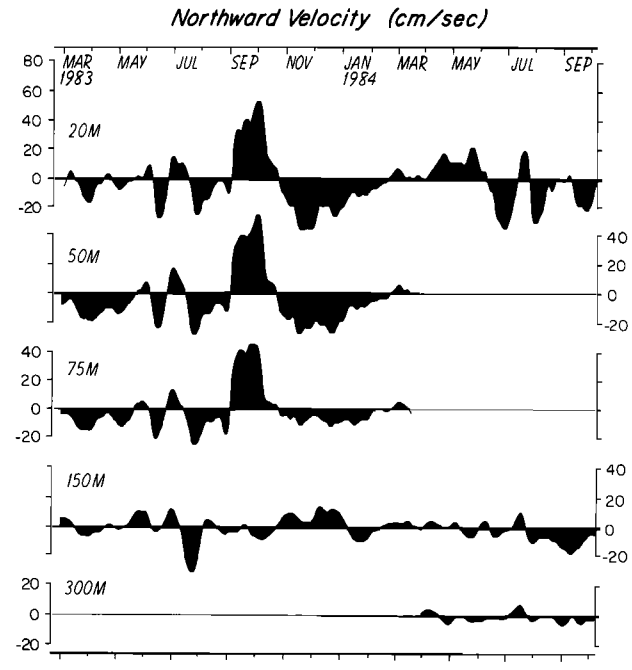

Fig. 17. Northward velocity time series from current meters.

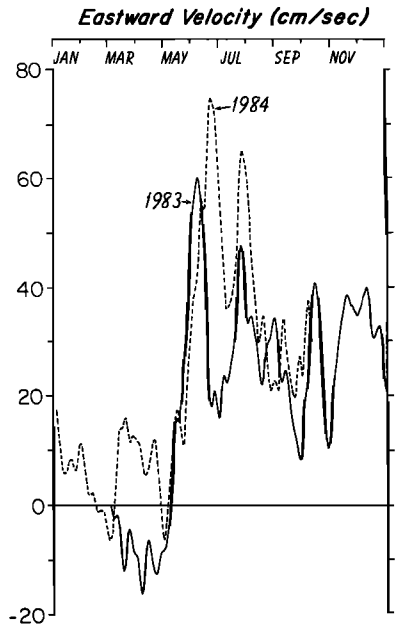

Fig. 18. Superposition of the 20-m eastward velocity for 1983 and 1984.

Northward velocity. The northward time series at 20 m has a low mean velocity of −2.8 cm/s and small (if any) seasonal variations. The record is dominated by a very energetic, 40-cm/s amplitude, ~6-month-long oscillation or event consisting of northward velocity in September and October 1983 and southward velocity from November 1983 to February 1984. This event, which occurred only at depths of 20–75 m, was not repeated in fall 1984. Since the records for 1983 and 1984 look

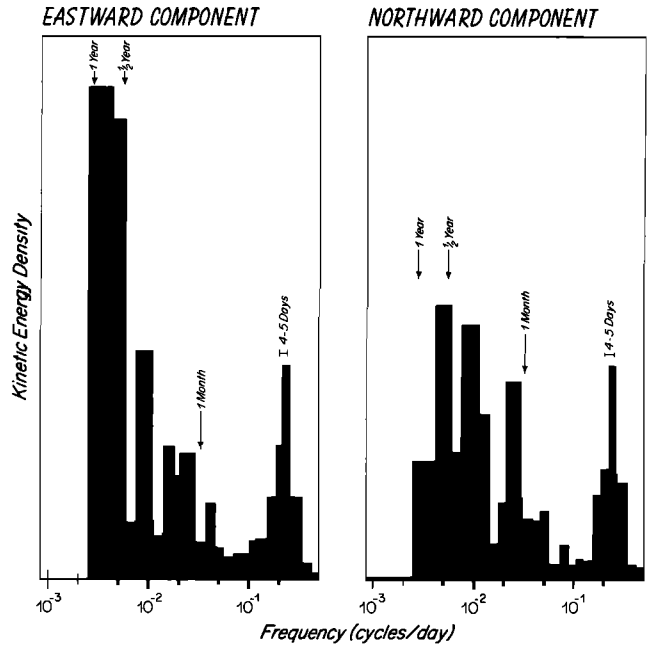

Fig. 19. Kinetic energy spectra of the eastward and northward velocity series measured at 20 m near 6°N, 28°W by current meter. Spectra are in energy-preserving form. Original series were low passed with a 2-day filter to suppress high-frequency oscillations.

very different and contain energetic high-frequency oscillations, it is not possible to resolve a climatological seasonal cycle for the northward velocity.

Eddy kinetic energy. The total eddy kinetic energy (EKE) from the current meter record at 20 m for u and v components was 245 cm^2/s^2 and 193 cm^2/s^2, respectively. The lowest frequency band, centered at a period of 590 days, contains little energy (Figure 19). This agrees with the longer ship drift series. Fifty percent of the total EKE of the u component is contained in the next two frequency bands, which include the annual and semiannual periods. Energy density gradually decreases at higher frequencies except for a peak at 3–6 days, the near-inertial frequency band containing 16% of the total energy. The rms amplitude of near-inertial oscillations is 8 cm/s, but values are intermittently much larger (up to 56 cm/s from one drifter near 8°N, 20°W). The spectrum calculated from the v component has a similar shape, but energy is lower at the annual period. A relatively large amount of energy is contained in the frequency band from periods of one to several months, corresponding to fluctuations apparent in the time series.

EKE was also calculated from buoys that drifted within a box surrounding the current meters, whose limits were 5°–7°N, 23°–33°W. The eastward and northward values from drifters are 280 cm^2/s^2 and 190 cm^2/s^2, very close to the values calculated from the 20 m current meter record given above. The EKE from both drifters and the current meter is larger than that from the 23-year average monthly ship drift series (107 cm^2/s^2) because the space-time averaging reduces the contribution from higher frequencies and smaller space scales.

The buoys reveal huge variations in EKE geographically and seasonally (Table 1). Values of EKE exceed 2000 cm^2/s^2 in the western NECC (40°–50°W) during fall, a result of fast speeds and the meanders there. During fall, the western NECC is as energetic as the Gulf Stream in the region 36°–40°N, 60°–70°W [*Richardson*, 1983]. During spring, the western NECC EKE drops to $\sim$100 cm^2/s^2. Along 28°W, values of EKE in the NECC are $\sim$400 cm^2/s^2 during fall and $\sim$200 cm^2/s^2 during spring.

The fall values in the eastern Pacific NECC at 3°–8°N, 100°–130°W, are $\sim$550, not very different from the eastern Atlantic NECC fall values [*Hansen and Paul*, 1984]. Pacific EKE peaks meridionally during fall near 2°–5°N $\sim$1700 cm^2/s^2 owing to instability waves [*Hansen and Paul*, 1984]. The few observations near 2.5°N in the Atlantic yield values less than this.

6. Meanders, Waves, and Eddies

The buoy and current meter records show three different kinds of oscillations, or waves, at frequencies between inertial and annual. The first are slowly propagating meanders of the western NECC, apparently caused by the North Brazil Current retroflecting into the western NECC. The second are energetic meridional oscillations of the eastern NECC (25°–30°W) during September 1983 to February 1984. The third are shorter-period, faster propagating waves which could be caused by an instability in the strong shear between the NECC and SEC (and perhaps between the SEC and the Equatorial Undercurrent). These waves were observed in the SEC in July, August, and September. They may also have been observed at 6°N in the NECC, although the time series there are more complicated. Part of the analysis of these three kinds of oscillations will be based on space- and time-lagged correlations of the buoy velocities (see the appendix).

Western NECC (30°–45°W)

Waves or meanders in the western NECC are seen in several buoy trajectories during fall (Figures 3, 4, and 5). The Lagrangian period and wavelength of these from a particularly clear example, buoy 52, were approximately 2 weeks and 700 km (Figure 7). This buoy and others show these waves to be largest and strongest in the west, with wavelengths of 900 km, meridional displacements of 300 km, and amplitudes of meridional velocity fluctuations of 100 cm/s. The collection of trajectories in the western NECC (30°–45°W), mainly from 1984, suggests that these waves slowly propagate westward with a phase speed of about 4 cm/s.

Fluctuations in the NECC were studied by calculating space- and time-lagged correlations from the buoy velocities (Figure 20, Table 2). The buoys were treated as if they were an array of current meters along the NECC. Their velocity measurements were grouped into space and time bins in order to examine fluctuations in a frame fixed with respect to the earth. The resulting correlation plots show how the dominant fluctuations would appear to moored current meters. The results agree with visual observations of trajectories composited in various ways. The western NECC during fall is dominated by oscillations with a characteristic wavelength of 910 km and (extrapolated) Eulerian period of 7.9 months, propagating slowly westward with a speed of about 4.3 cm/s (Table 2). The Eulerian period is the time required for a wave to pass a fixed point. This is longer than the Lagrangian period, the time for a buoy to drift through a wave, especially when the buoys are drifting rapidly in an opposite direction to the wave's phase propagation.

This same pattern of slowly propagating meanders is observed in model simulations of the Atlantic NECC, although the model meanders have a shorter wavelength and move more slowly than was observed here [*Philander and Pacanowski*, 1986*a*]. The contoured correlation matrix from model simulations looks very much like that from the drifters; the model wavelength is 590 km and the waves propagate westward at 1.2 cm/s (Figure 20, Table 2). In the model the westward phase propagation is most apparent during October–February, but there is an indication of continued westward propagation of these meridional oscillations into spring, in accord with the drifter observations then.

We suggest that the cause of the meanders is the swift North Brazil Current that retroflects into the western NECC by first overshooting the NECC to the north near 50°W, 10°N; then dipping southward near 45°W, 5°N; and finally establishing a quasi-stationary meander pattern or Rossby wave wake about some mean latitude. Stationary Rossby waves in an eastward current have an approximate wavelength given by $2\pi(u/\beta)^{1/2}$ [*Pedlosky*, 1979]. This amounts to 840 km using values appropriate to the NECC, $u = 41$ cm/s (Table 1), and β evaluated at 6°N. The slowly propagating oscillations observed with drifters (and model simulations) appear to be a gradual westward shifting of these meanders or waves as the NECC decreases in speed during fall and winter.

The model-simulated time series also show instability waves at 6°N [*Philander et al.*, 1986]. However, the instability waves are not seen in the correlation matrix for this region unless the series have been previously high passed. The reason that we

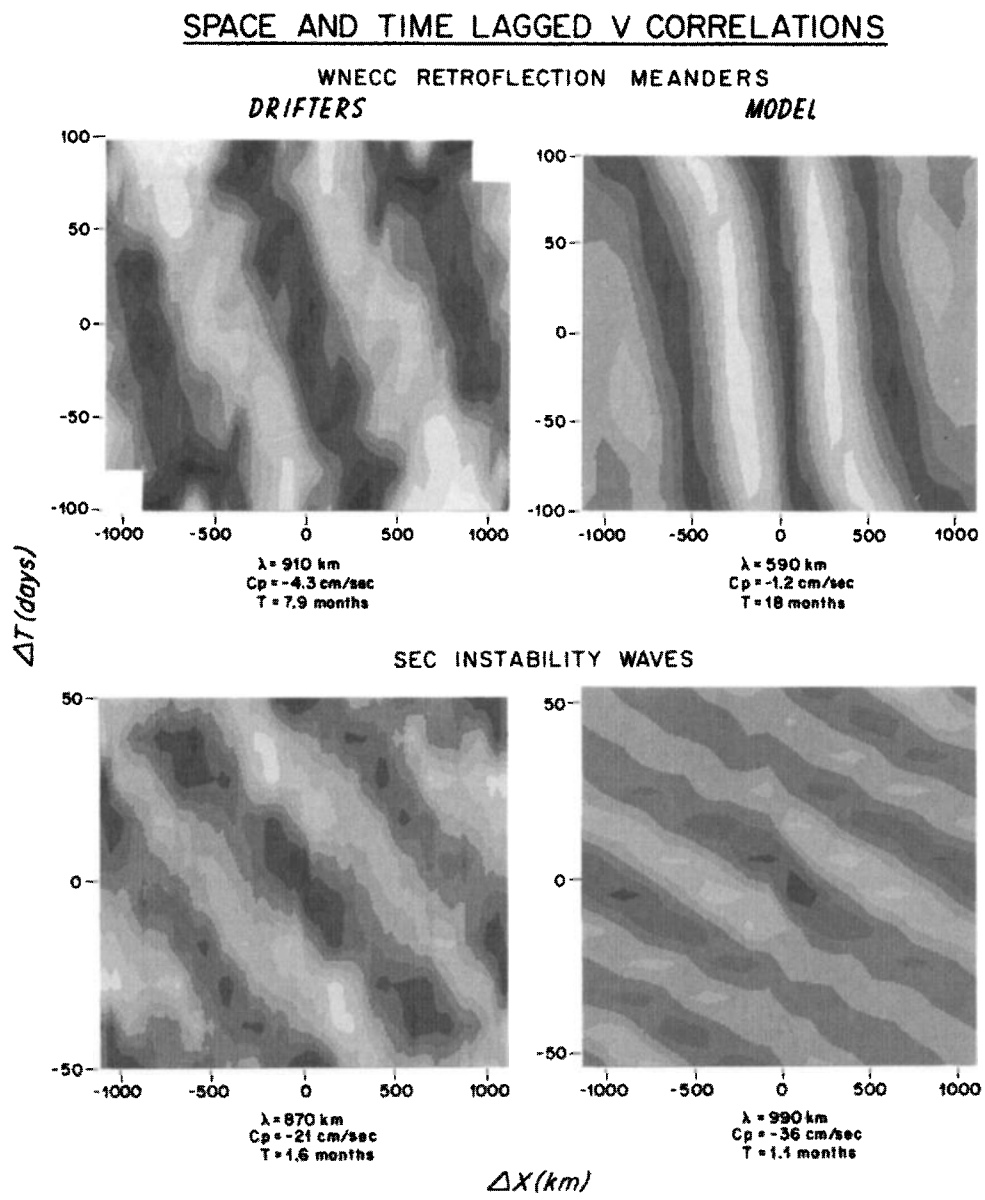

Fig. 20. Lagged time and space correlation matrix calculated from drifting buoys in the western NECC, 3°–8°N, 30°–45°W, during July–November of 1984 and in the SEC, 2°–8°S, 10°–30°W, July–August 1984. Correlations are also shown for model simulations in the western NECC (6°N, 30°–45°W, October–December) and in the SEC (4°S, 20°–35°W, July–August). Shading is darkest for the highest correlations and lightest for the lowest correlations. The spacing between ridges of high correlation and their orientation give estimates of wavelength, period, and phase velocity of the dominant fluctuations (Table 2).

do not see the instability waves in the western NECC may be that their amplitude is dwarfed by the large amplitude of the slower, more energetic, meanders.

Eastern NECC (20°–35°W)

During fall 1983 and spring 1984, an unusually strong meridional oscillation was recorded by current meters (Figure 17) and drifting buoys (Figure 21). Five drifters were launched in the NECC in early September along 28°W at 4°, 5°, 6°, 7°, and 8°N. The four southern ones initially moved northward, in agreement with the current meter record. One buoy launched at 5°N, 28°W was trapped for nearly 3 months in a closed clockwise circulation centered near 6°N, 26°W. The period of its loops was about 24 days, the average swirl speed was 20 cm/s, and the diameter was about 150 km. Three other buoys from 4°N, 6°N, and 7°N were deflected around this feature with typical speeds of 30–50 cm/s, in patterns indicating a diameter of about 300 km. The implied drift of the feature from the buoys and current meter is eastward at a few centimeters per second. Lagged space and time correlations were calculated for September–November; the dominant fluctuations had a wavelength of 480 km and an eastward phase velocity of 2.2 cm/s, generally agreeing with trajectories and velocities series.

The energetic meridional oscillations of this event occurred when the NECC was gradually slowing. At this time the eastward flow seemed to be severely disrupted. Two buoys in the western NECC were expelled from it at 30°W: one was twice sidetracked southward into the SEC, in September and again in November; the other buoy was sidetracked northward into the NEC in October.

TABLE 2. Characteristics of the Dominant Fluctuations From Space- and Time-Lagged Correlations

Region	Time	$\bar{u}$, cm/s	$\bar{v}$, cm/s	Wavelength, km	Period, months	Eastward Phase Velocity, cm/s
		Drifter Data				
WNECC (3°–8°N, 30°–45°W)	July–Nov. 1984	26.4	8.8	910	(7.9)	−4.3
ENECC (event) (3°–10°N, 20°–35°W)	Sept.–Nov. 1983	17.6	−2.0	480	(8.2)	+2.2
SEC (2°S–8°S, 10°–30°W)	July–Aug. 1984	−31.3	−1.2	870	1.6	−21
		Model Simulations				
WNECC (6°N, 30°–45°W)	Oct.–Dec.	21.3	13.1	590	(18)	−1.2
SEC (4°S, 20°–35°W) high-passed data	July–Aug.	−59.1	−4.7	990	1.1	−36

Values of $\bar{u}$ and $\bar{v}$ are averages over the whole region and time. Wavelength, period, and phase velocity are estimated from the lagged space and time correlation matrix (see Figure 20 and appendix). Values of wavelength and period are the distances in longitude and time between parallel ridges of high correlations. Parentheses indicate values inferred from extrapolations of the data. Phase velocity is determined from the orientation of the ridges of high correlation. Model simulations of the 5-m velocity field were obtained from *Philander and Pacanowski* [1986*a*] and analyzed here to compare characteristics. The simulated time series contains values at 3-day intervals and 1° longitude separations. The original series were used as were a high-passed subset that contained only the ~ 30-day instability waves.

The oscillation may have been an unusually energetic western NECC meander that had propagated eastward into this region. Such an event may occur only occasionally near 28°W: no other oscillation of this magnitude had begun by October 12, 1984, when the mooring was recovered. Another similar and extremely strong meridional velocity occurred in October 1984 near 38°W, when one buoy shot northward with a speed of 100 cm/s from the SEC across the mean position of the NECC and into the NEC (Figure 4), and another buoy that had been rapidly drifting eastward in the NECC was sidetracked northward into the NEC near 38°W. These disruptions show that the NECC is at times less continuous than is implied by average ship drift maps. No such events are seen in model simulations [*Philander and Pacanowski*, 1986*a*], but the model was forced by monthly averaged winds, precluding year-to-year variability and perhaps such strong events.

During June–August each year, the 20-m current meter recorded meridional oscillations with a characteristic amplitude of 20 cm/s and period of 35 days (Figure 17). Although in 1983 these were eclipsed by the event in September, in 1984 they continued into September.

Superimposed on the seasonal changes in u velocity of the NECC are higher-frequency oscillations (Figure 16). The largest ones occur in June and July of both years and extend into November in 1983. The period and amplitude of these are approximately 40 days and 15 cm/s, similar to v fluctuations then. The u and v components appear to be 90° out of phase and to rotate clockwise. The appearance of these fluctuations during summer and their period suggest again that they could be instability waves. However, their period and propagation characteristics differ somewhat from those measured by current meters near the equator [*Weisberg*, 1984*b*] and seen in infrared images in 1983 [*Legeckis and Reverdin*, 1987]. These Eulerian fluctuations cannot be just an effect of meridional advection of the high-velocity core of the NECC passing the current meters, which could cause zonal oscillations at a period of one-half the period of the meanders.

SEC

As the SEC buoys drifted westward, they meandered in a north-south direction (Figures 3 and 4). The meanders appear to have maximum meridional displacements during July–September of both years. (Monthly EKE values in the SEC calculated from ship drifts also peak during July–September.) Synoptic composites of the trajectories and space-time correlations of the meridional velocities reveal the meanders to have a wavelength of 870 km, Eulerian period of 48 days, and westward phase speed of 21 cm/s (Figure 20, Table 2). These waves could be generated by an instability of the swift SEC or by wind forcing at 35- to 50-day periods, as was discussed by *Colin and Garzoli* [1987].

Discussion of Instability Waves

Model simulations of instability waves in the Atlantic are described by *Philander and Pacanowski* [1986*a*], and *Philander et al.* [1986]. These waves appear in June and July centered near 1°N and have periods of 20–30 days, wavelengths of 500–1000 km, and westward phase speeds of 30–50 cm/s. They continue into fall gradually decreasing in amplitude.

Confirmation of instability waves in the equatorial Atlantic comes from current meters [*Weisberg*, 1984*b*], satellite infrared images [*Legeckis and Reverdin*, 1987] and shipboard measurements [*McPhaden et al.*, 1984]. The current meter records near the equator agree closely with the model simulations in showing a burst of meridional velocity fluctuations in June–July 1983 and 1984. During June–July 1983 the period of the waves was 25 days, the wavelength was 1140 km, the velocity amplitude was 65 cm/s (twice the model value), and the phase velocity was westward at 53 cm/s [*Weisberg*, 1984*b*]. The oscillations continued from June 1983 to February 1984, but after July their period increased to about 40 days and their amplitude gradually decreased (R. W. Weisberg, personal communication, 1986). Meridional displacements of the sea surface temperature front extended from 2°S to 6°N (10°W–20°W), clearly showing the large displacement

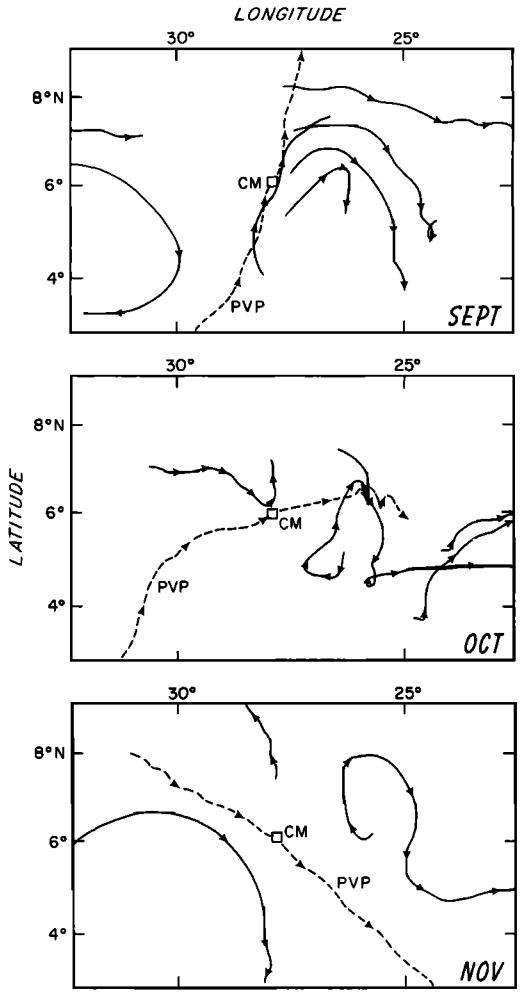

Fig. 21. Buoy trajectories and progressive vector plot (PVP) of the 20-m current meter series showing details of the energetic meridional oscillation which occurred near 28°W during fall 1983. Arrowheads are spaced at 5-day intervals. The location of the current meter is shown by the small box near 6°N, 28°W.

amplitudes of these waves in 1983 [*Legeckis and Reverdin*, 1987].

The current meter records at 6°N and the buoy trajectories in the SEC generally agree with the model simulations of instability waves and the data closer to the equator. The wavelength, period, and phase propagation of the model and observed waves are similar (but not identical), and the timing coincides: the burst of waves in summer and their decreasing period, phase speed, and amplitude during fall. One difference is that the observed velocity amplitude at 6°N is 20 cm/s in July–August versus the model's amplitude of ~5 cm/s.

7. Summary

Buoys in the SEC south of the equator drifted westward, turned northward into the North Brazil Current, and accelerated up to the highest speeds recorded, ~167 cm/s. Most of these buoys, however, grounded on the coast of Brazil. These plus a few buoys north of the equator show that in spring the North Brazil Current continues up the coast into the Guyana Current and Caribbean. A major finding is that during fall the whole North Brazil Current (measured by five drifters) veers offshore or retroflects, forming the western NECC. This is a key factor in the modulation of northward heat flux across 8°N [see *Philander and Pacanowski*, 1986*b*]. During fall, the NECC flows eastward across th Atlantic into the Guinea Current. About half the buoys in the NECC eventually entered the Guinea Current, and about half entered the NEC. Some buoys were expelled from the NECC, indicating that the eastward flow is not always continuous. During spring and west of 20°W the NECC disappears and is replaced by westward flow. Buoys that left the NECC and entered the NEC drifted westward to the Caribbean with little seasonal variation.

Near 28°W, where the data are most numerous, the seasonal variation of the NECC was very regular from year to year, based on drifters and ship drifts. The amplitude of the seasonal variation in eastward velocity from drifters, current meters, and ship drifts is 15–20 cm/s. The largest seasonal variations were observed in the western NECC owing to both a faster eastward velocity in fall and a faster westward velocity in spring.

During July–August 1984 at 6°N, 28°W, the NECC extended to a depth of ~350 m. A maximum eastward volume transport at that time was estimated to be 54×10^6 m^3/s by combining a meridional profile of velocity from drifters with a vertical profile from current meters. This is probably an overestimate due to the lack of subsurface velocity at other latitudes. In spring the subsurface NECC (at 6°N) vanished, although large fluctuations in velocity persisted.

Some NECC near-surface water is inferred to descend out of the surface layer and to flow equatorward. The transport of downwelled water from the near-surface convergence was estimated to be 8×10^6 m^3/s (by multiplying annual ship drift velocities by a mixed layer depth of 30 m). At 6°N, 28°W, the mean equatorward velocity peaked at ~6 cm/s at a depth of 50 m. The transport of equatorward flow was estimated to be about 14×10^6 m^3/s. These values of transport are consistent with model simulations of equatorial circulation [*Philander and Pacanowski*, 1986*b*].

Energetic fluctuations with periods of a few months and amplitudes of 20–40 cm/s are superimposed on the lower frequency annual variations. The most energetic region of the tropical Atlantic is the North Brazil Current–western NECC [*Wyrtki et al.*, 1976; *Richardson and McKee*, 1984]. The eddy kinetic energy in the western NECC as measured by drifters reached 2400 cm^2/s^2, comparable to the high EKE region in the Gulf Stream. The high EKE is due to the swift North Brazil Current retroflecting into the western NECC, forming meanders there. The resulting meanders of the western NECC have a wavelength of 900 km, meridional displacements of 300 km, and an amplitude of meridional velocity up to 100 cm/s. The meanders slowly propagate westward during fall with a phase speed of 4 cm/s.

During September 1983 to March 1984, one very energetic meridional oscillation of amplitude 40 cm/s was observed in the current meter series. This event could have been an unusually energetic meander propagating in from the west. The feature drifted eastward at 2 cm/s and had a wavelength of 480 km. Another observation of a strong meridional velocity and a disruption of the NECC was observed in October 1984 near 38°W.

Oscillations in the SEC during July–September may be due to instability waves generated in the strong shear between the NECC and SEC. These waves have a wavelength of 870 km, an Eulerian period of 48 days, and a westward phase speed of 21 cm/s. Velocity oscillations of 15–20 cm/s and 35- to 40-day

period were observed in the current meter records (6°N, 28°W) during June–August each year. These oscillations are also inferred from their characteristics to be instability waves, but they are difficult to identify because of energetic oscillations in the NECC from other causes, such as the seasonal cycle, retroflection meanders, and the event described above. The observed waves in the SEC (and at 6°N, 28°W) and instability waves have similar (but not equal) wavelengths, periods, phase velocities, and timing; a burst of waves appears during summer when the SEC-NECC shear is largest.

Energetic inertial oscillations were observed in the NECC with an rms amplitude of 8 cm/s at 6°N, 28°W. Occasionally, much larger amplitudes occur.

8. Conclusions

The collection of drifter trajectories from SEQUAL and FOCAL provide a description of the Lagrangian circulation in the equatorial Atlantic including estimates of seasonal variations, the connection between different currents, and details of meanders and oscillations in the NECC and SEC. Where measurements are dense, the agreement tends to be good between space-time average velocities from drifters and ship drifts. This suggests that (1) the drifter measurements are representative of rather typical conditions, and (2) ship drifts have given a good portrayal of climatology. Some differences were noted. Velocities from drifters and a current meter at 20 m also agree well for close passes, enabling us to relate velocity series at a point in the NECC to space-time average velocities from drifters and ship drifts. Probably the biggest deficiencies in the data are the lack of subsurface velocity series at more than one point in the NECC and the lack of many surface and any subsurface velocities in the energetic western NECC. A forthcoming study of the merged SEQUAL-FOCAL data may reveal additional information about the subsurface and western NECC.

Appendix: Definition of Statistical Operations Used in This Paper

Box Averages

Drifting buoys were treated as mobile current meters that give velocity measurements along their paths. These individual drifter (and ship drift) velocities were grouped into space and time boxes to calculate characteristic mean velocities. Boxes were chosen both along and across the NECC and average velocity profiles calculated. A large box spanning the whole NECC near 28°W was used to calculate a time series of monthly average values. In each box we calculated the mean velocity $\bar{u}$, $\bar{v}$ in x and y directions, the departures u', v' from this mean, variances $\langle u'u' \rangle$, $\langle v'v' \rangle$ and eddy kinetic energy EKE $= \frac{1}{2}(\langle u'u' \rangle + \langle v'v' \rangle)$.

The standard error of the mean velocity was estimated using the following relationship:

$$\text{standard error of } \bar{u} = \left[\frac{\langle u'u' \rangle}{[(N/\tau) + n]} \right]^{1/2}$$

where $\langle u'u' \rangle$ is the variance, N is the number of days of velocity observations, τ is the integral time scale (days) of the autocorrelation function, and n is the number of different buoys which are assumed to be uncorrelated. From the 20-m current meter record at 6°N, 28°W τ was estimated to be 22 days in the zonal direction and 12 days in the meridional direction. These are estimates of the time required at a point for an independent observation of velocity.

Lagged Space and Time Correlations

In order to estimate space and time scales and phase propagation of the dominant fluctuations, lagged space and time correlations were calculated using the buoy locations and velocities. First, the mean velocity was calculated in a space-time box encompassing the relevant subset of trajectories. The mean velocity was then subtracted from each of the individual measurements. Pairs of the residual velocities were multiplied together and grouped into lagged space and time bins. Average correlations were calculated for each bin using

$$\rho = \frac{\langle V_1' V_2' \rangle}{[\langle V_1' V_1' \rangle \langle V_2' V_2' \rangle]^{1/2}}$$

where $V_1'(x, t)$ is the residual velocity at one time and location, and $V_2'(x + \Delta x, t + \Delta t)$ is the residual velocity at another time and location. The resulting correlation matrix was then plotted and contoured. Analysis concentrated on the northward velocity because the mean northward velocity and its spatial gradients are small and because large-amplitude fluctuations are seen in it. Eastward velocity fluctuations are complicated by the large-scale horizontal shear across the NEC, NECC, and SEC and zonal variations of these currents. Time periods were chosen when the currents were nearly steady on a seasonal time scale.

Acknowledgments. Funds were provided by the National Science Foundation (grants OCE82-17112 and OCE82-08744) and by the Institut Français de Recherche pour l'Exploitation de la Mer in Brest, France, and Programme National d'Etude de la Dynamique des Climats, Paris. This work would not have been possible without the leadership of SEQUAL chairmen Mark Cane and Eli Katz and helpful collaboration with the other SEQUAL and FOCALnauts. The WHOI Buoy Group prepared the current meters, and the North Carolina State University Group deployed and recovered the moorings. Many SEQUAL and FOCAL participants helped to deploy buoys and moorings from the R/V *Capricorne*, R/V *Conrad*, R/V *Gyre*, R/V *Knorr*, R/V *Marion Dufresne*, and R/V *Nizery*. Chief scientists were Christian Colin, Michèle Fieux, Christian Hénin, Philippe Hisard, Eli Katz, Bernard Piton, and Robert Weisberg. Data were processed and results calculated and plotted by Christine Wooding, Ellen Levy, Theresa McKee, and David Walsh. George Philander and Ronald Pacanowski generously provided their model simulations. The manuscript was typed by Mary Ann Lucas and the figures drawn by Ruth Davis and Kimberly Sikora. A draft of this paper was written while P.L.R. was a visiting scholar at the Scripps Institution of Oceanography, La Jolla, California; Lawrence Armi helped arrange the visit. Gabriel Csanady and Susan Schwartz made helpful suggestions on an earlier version of this paper. Woods Hole Oceanographic Institution contribution 6297.

References

Boisvert, W. E., Major currents in the North and South Atlantic oceans between 64°N and 60°S, *Tech. Rep. TR-193*, 105 pp., Nav. Oceanogr. Office, Bay Saint Louis, Miss., 1967. (Available as NTIS AD-827-58619 from Natl. Tech. Inf. Serv., Springfield, Va.)

Bruce, J. G., J. L. Kerling, and W. H. Beatty III, On the North Brazilian Eddy Field, *Prog. Oceanogr.*, *14*, 57–63, 1985.

Bubnov, V. A., and V. D. Egorikhin, Study of water circulation in the tropical Atlantic, *Deep Sea Res.*, *26*, GATE suppl. II, 125–136, 1979.

Bubnov, V. A., V. M. Vasilenko, and L. M. Krivelevich, The study of low-frequency variability of currents in the tropical Atlantic, *Deep Sea Res.*, *26*, GATE suppl. II, 199–216, 1979.

Cochrane, J. D., F. J. Kelley, Jr., and C. R. Olling, Subthermocline countercurrents in the western equatorial Atlantic Ocean, *J. Phys. Oceanogr.*, *9*, 724–738, 1979.

Colin, C., and S. L. Garzoli, In situ wind measurements and the ocean

response in the equatorial Atlantic during the Programme Français Océan et Climat dans l'Atlantique Equatorial Seasonal Response of the Equatorial Atlantic Experiment, *J. Geophys. Res.*, in press, 1987.

Garzoli, S. L., and E. J. Katz, The forced annual reversal of the Atlantic North Equatorial Countercurrent, *J. Phys. Oceanogr.*, *13*, 2082–2090, 1983.

Halpern, D., Variability of near-surface currents in the Atlantic North Equatorial Countercurrent during GATE, *J. Phys. Oceanogr.*, *10*, 1213–1220, 1980.

Hansen, D. V., and C. A. Paul, Genesis and effects of long waves in the equatorial Pacific, *J. Geophys. Res.*, *89*, 10,431–10,440, 1984.

Katz, E. J., R. L. Molinari, D. E. Cartwright, P. Hisard, H. U. Lass, and A. deMesquita, The seasonal transport of the equatorial undercurrent in the western Atlantic (during the Global Weather Experiment), *Oceanol. Acta*, *4*, 445–450, 1981.

Legeckis, R., and G. Reverdin, Long waves in the equatorial Atlantic Ocean during 1983, *J. Geophys. Res.*, *92*, 2835–2842, 1987.

Levy, E., and P. L. Richardson, Moored current meter data from the Atlantic North Equatorial Countercurrent near 6°N, 28°W (March–October 1984), vol. XXXVII, *Tech. Rep. WHOI-85-7*, 49 pp., Woods Hole Oceanogr. Inst., Woods Hole, Mass., 1985.

McPhaden, M. J., M. Fieux, and J. Gonella, Meanders observed in surface currents and hydrography during an equatorial Atlantic transect, *Geophys. Res. Lett.*, *11*, 757–760, 1984.

Molinari, R. L., Satellite-tracked drifting buoy observations of near-surface currents and temperature in the central and western tropical Atlantic Ocean, *J. Geophys. Res.*, *88*, 4433–4438, 1983.

Muller-Karger, F. E., C. R. McClain, and D. K. Clark, The fate of the Orinoco and Amazon River plumes as observed in a CZCS time series (abstract), *Eos Trans. AGU*, *67*, 1056, 1986.

Neumann, G., Seasonal salinity variations in the upper strata of the western tropical Atlantic Ocean, I, Sea surface salinities, *Deep Sea Res.*, *16*, suppl., 165–177, 1969.

Patzert, W. C., and G. J. McNally, Surface current variability in the tropical Pacific during 1979 and 1980 using drifting buoys, in *Recent Progress in Equatorial Oceanography: A Report of the Final Meeting of SCOR Working Group 47*, pp. 151–156, N.Y.I.T. Press, Fort Lauderdale, Fla., 1981.

Payne, R. E., Surface wind measurements in SEQUAL I, *Geophys. Res. Lett.*, *11*, 719–721, 1984.

Pedlosky, J., *Geophysical Fluid Dynamics*, 624 pp., Springer, New York, 1979.

Perkins, H., and J. Van Leer, Simultaneous current-temperature profiles in the Equatorial Countercurrent, *J. Phys. Oceanogr.*, *7*, 264–271, 1977.

Perlroth, I., The distribution of water type structure in the first 300 feet of the equatorial Atlantic, in *Proceedings of the Symposium on Oceanography and Fisheries Resources of the Tropical Atlantic: Abidjan, Ivory Coast*, pp. 185–191, United Nations Educational, Sicentific and Cultural Organization, Paris, 1966.

Philander, S. G. H., and R. C. Pacanowski, A model of the seasonal cycle in the tropical Atlantic Ocean, *J. Geophys. Res.*, *91*, 14,192–14,206, 1986*a*.

Philander, S. G. H., and R. C. Pacanowski, The mass and heat budget in a model of the tropical Atlantic Ocean, *J. Geophys. Res.*, *91*, 14,212–14,220, 1986*b*.

Philander, S. G. H., W. J. Hurlin, and R. C. Pacanowski, Properties of long equatorial waves in models of the seasonal cycle in the tropical Atlantic and Pacific Oceans, *J. Geophys. Res.*, *91*, 14,207–14,211, 1986.

Piton, B., and F.-X. Fusey, Trajectories of two satellite-tracked buoys in the Gulf of Guinea, July 1978–July 1979, *Trop. Ocean-Atmos. Newsl. 10*, pp. 5–7, Joint Inst. for the Study of the Atmos. and Oceans, Univ. of Wash., Seattle, 1982.

Reverdin, G., and A. Kartavtseff, Bouées FOCAL, Mai 1983–October 1984, Recueil des trajectoires et séries temporelles, report, 120 pp., Lab. d'Océanogr. Phys., Mus. Natl. d'Hist. Nat., Paris, 1984.

Reverdin, G., and M. J. McPhaden, Near-surface current and temperature variability observed in the Equatorial Atlantic from drifting buoys, *J. Geophys. Res.*, *91*, 6569–6581, 1986.

Reverdin, G., J. Gonella, M. Fieux, and M. J. McPhaden, Temperature variations in the equatorial Atlantic as revealed by drifting buoys, *Geophys. Res. Lett.*, *11*, 791–794, 1984.

Richardson, P. L., Eddy kinetic energy in the North Atlantic from surface drifters, *J. Geophys. Res.*, *88*(C7), 4355–4367, 1983.

Richardson, P. L., Drifting buoy trajectories in the Atlantic North Equatorial Countercurrent during 1983, *Geophys. Res. Lett.*, *11*, 745–748, 1984*a*.

Richardson, P. L., Moored current meter measurements in the Atlantic North Equatorial Countercurrent during 1983, *Geophys. Res. Lett.*, *11*, 749–752, 1984*b*.

Richardson, P. L., and T. K. McKee, Average seasonal variation of the Atlantic equatorial currents from historical ship drifts, *J. Phys. Oceanogr.*, *14*(7), 1226–1238, 1984.

Richardson, P. L., and D. Walsh, Mapping climatological seasonal variations of surface currents in the tropical Atlantic using ship drifts, *J. Geophys. Res.*, *91*, 10,537–10,550, 1986.

Richardson, P. L., and C. M. Wooding, Surface drifter measurements in the Atlantic North Equatorial Countercurrent 1983–1985, *Tech. Rep. WHOI-85-31*, 130 pp., Woods Hole Oceanogr. Inst., Woods Hole, Mass., 1985.

Schumacher, A., Monatskarten der Oberflächenströmungen im Nordatlantischen Ozean, *Ann. Hydrogr. Mar. Meteorol.*, *68*, 109–123, 1940.

Schumacher, A., Monatskarten der Oberflächenströmungen im äquatorialen und sudlichen Atlantischen Ozean, *Ann. Hydrogr. Mar. Meteorol.*, *71*, 219–219, 1943.

Weisberg, R. H., Instability waves observed on the equator in the Atlantic Ocean during 1983, *Geophys. Res. Lett.*, *11*, 753–756, 1984*b*.

Weisberg, R. H., Seasonal adjustments in the equatorial Atlantic during 1983 as seen by surface moorings, *Geophys. Res. Lett.*, *11*, 733–735, 1984*a*.

Weisberg, R. H., Instability waves observed on the equator in the Atlantic Ocean during 1983, *Geophys. Res. Lett.*, *11*, 753–756, 1984*b*.

Wyrtki, K., L. Magaard, and J. Hager, Eddy energy in the ocean, *J. Geophys. Res.*, *81*, 2641–2646, 1976.

P. L. Richardson, Woods Hole Oceanographic Institution, Woods Hole, MA 02543.

G. Reverdin, Laboratoire d'Océanographie Dynamique et de Climatologie, Université Paris VI, Tour 14, 4 place Jussieu, 75252 Paris Cedex 05, France.

(Received August 29, 1986;
accepted February 12, 1987.)